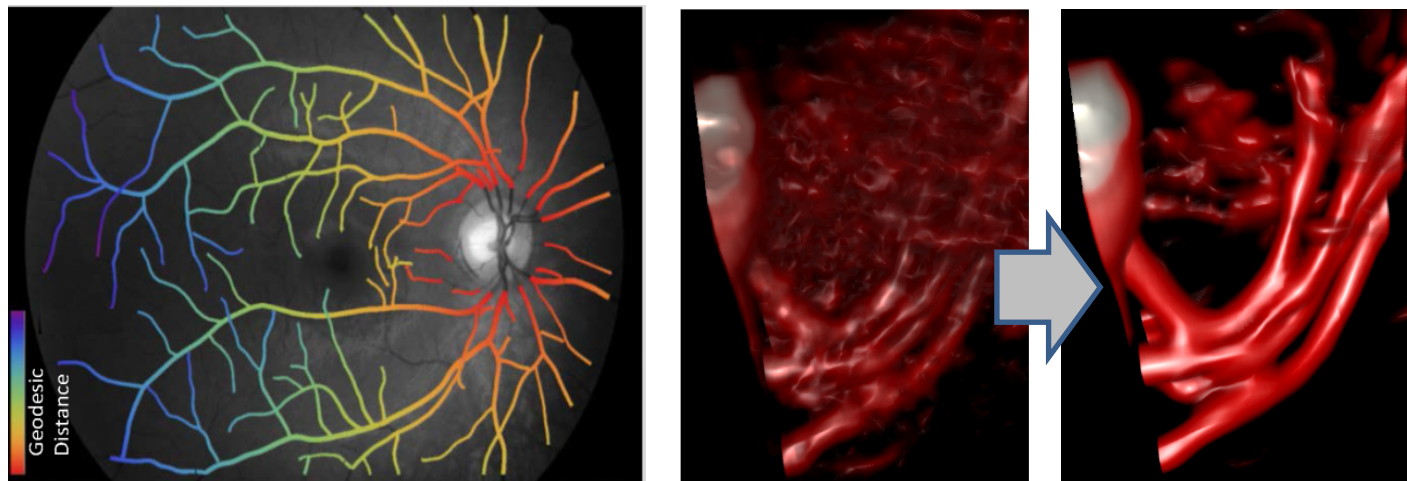


PDEs on the Homogenous Space of Positions and Orientations

Remco Duits

TU/e Eindhoven

E.J. Bekkers, J.-M. Mirebeau, J.M. & J.W. Portegies, A. Mashtakov.

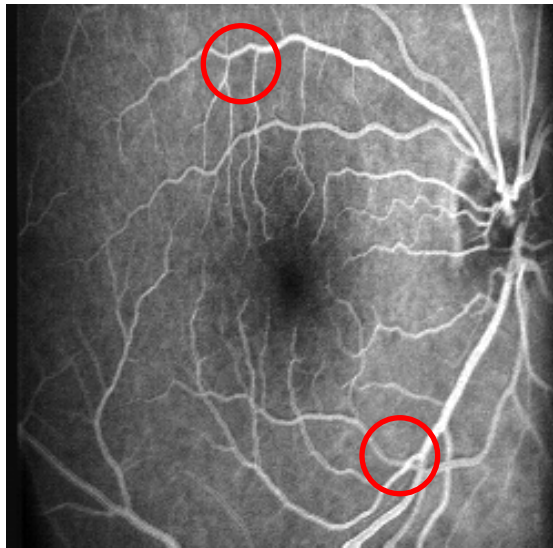


Project: ERC Lie Analysis
335555

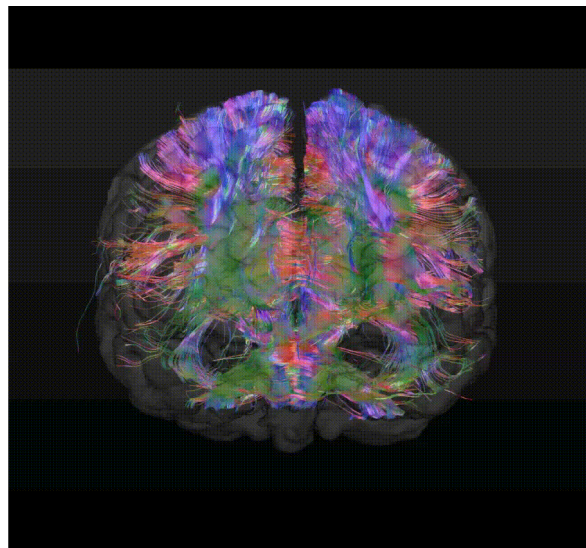


Background

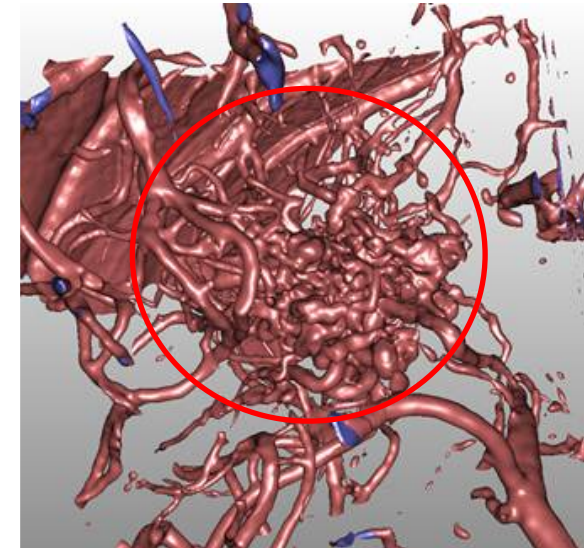
- Elongated structures appear in many medical images



Retina



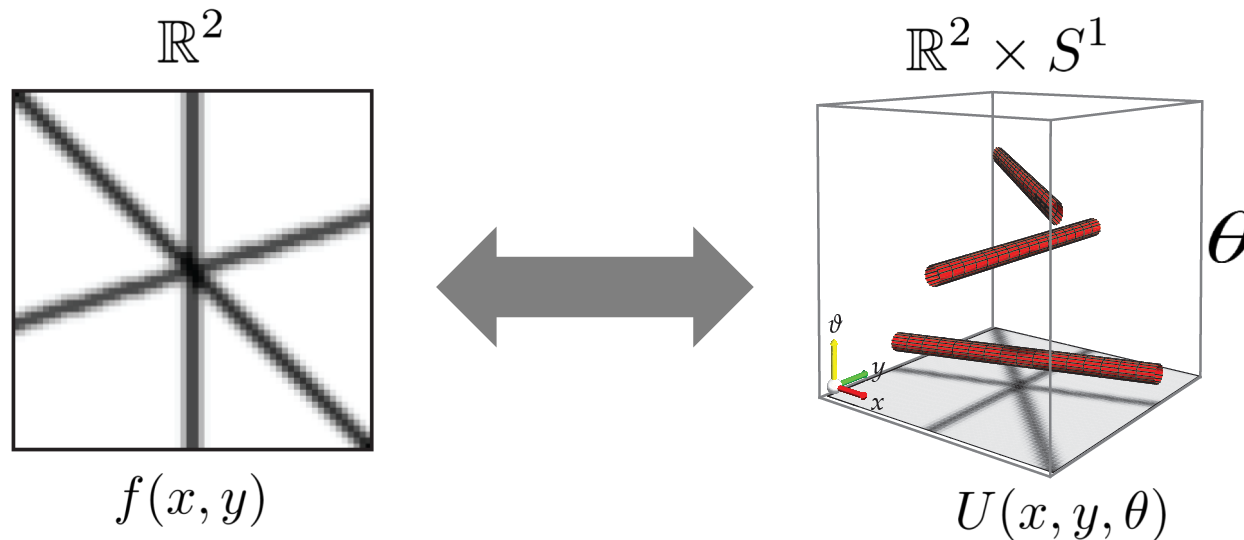
Brain White Matter



Vessels in brain

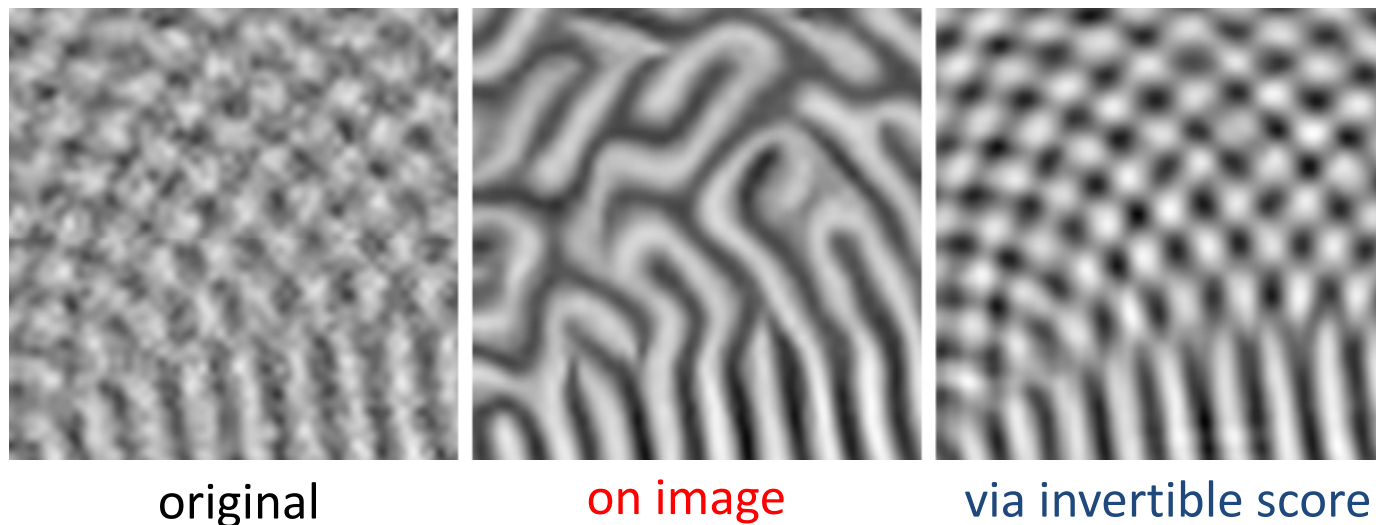
- Current detection and enhancement often fails at crossings/bifurcations etc.
- a costly increase of user-interaction in tracking tools for computer aided diagnosis & therapy planning

Solution: Extend the Domain of Images



PhD thesis 2005, IJCV 2007 Duits: invertible orientation scores, image reps on $\mathbb{R}^2 \times S^1$

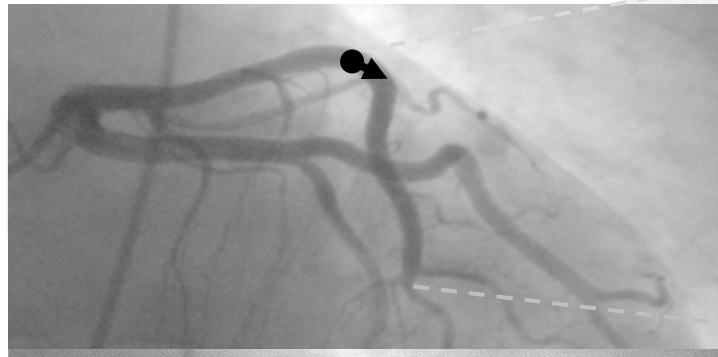
1.) For correct enhancement, e.g. crossing-preserving diffusions:



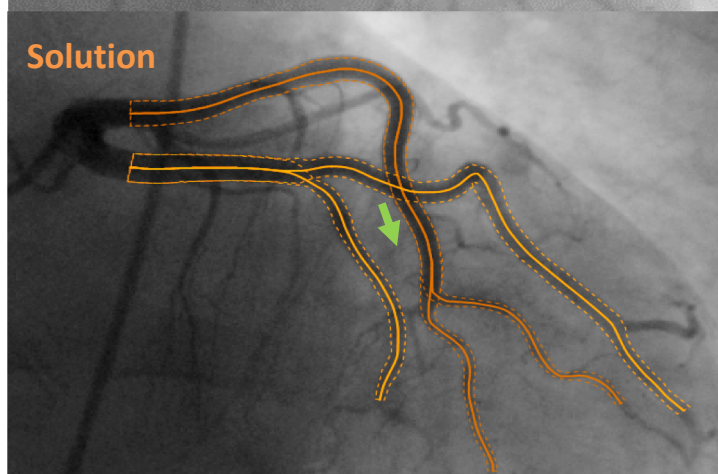
Solution: Extend the Domain of Images

2.) For correct tracking at crossings and bifurcations:

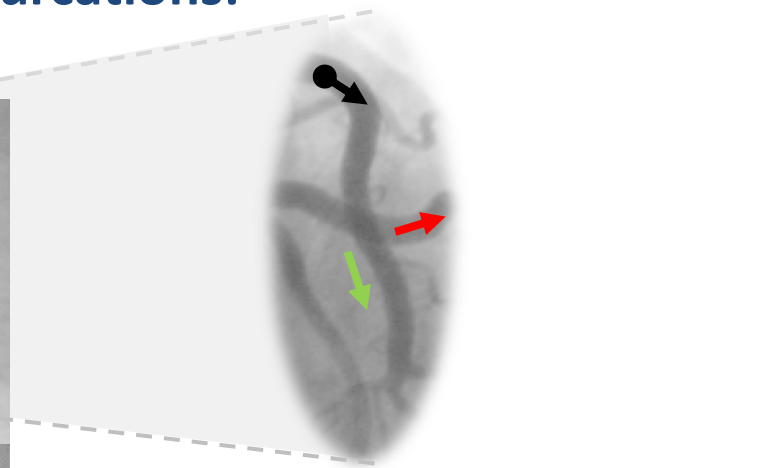
Vessel tracking in 2D X-ray angiogram



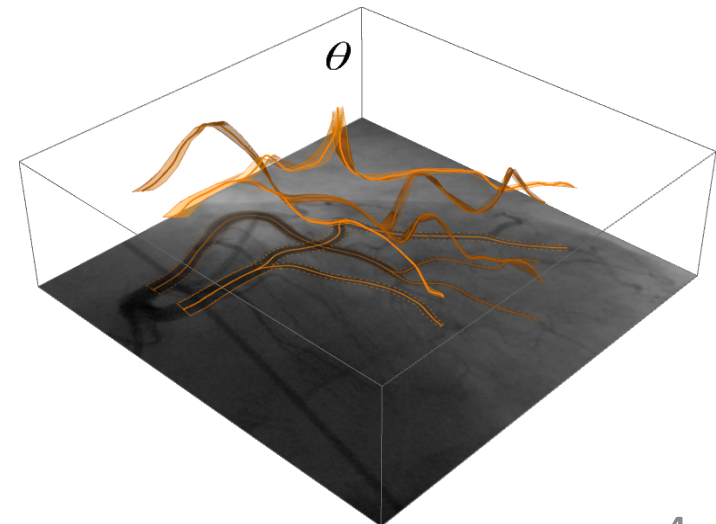
Problems
with
industrial
tracker



Solution



Vessel tracking in
orientation scores



Lie Group and Score

Lie group: differentiable manifold with group product s.t. $(g, h) \mapsto g^{-1}h$ is smooth

Unitary Representation $\mathcal{U}_{g_1 g_2} = \mathcal{U}_{g_1} \mathcal{U}_{g_2}$ and $\mathcal{U}_g^* = \mathcal{U}_{g^{-1}}$

E.g.

$$(\mathcal{U}_g f)(\mathbf{y}) = f(\mathbf{R}^{-1}(\mathbf{y} - \mathbf{x})), \quad g = (x, \mathbf{R}) \in SE(d)$$

Lie group $G = \text{SE}(d)$: $g_1 g_2 = (\mathbf{x}_1, \mathbf{R}_1) (\mathbf{x}_2, \mathbf{R}_2) = (\mathbf{x}_1 + \mathbf{R}_1 \mathbf{x}_2, \mathbf{R}_1 \mathbf{R}_2)$

In image analysis:

- image: f

- kernel: ψ

- **Score:** $\widetilde{\mathcal{W}}_\psi f(g) = \int_{\mathbb{R}^d} \overline{\mathcal{U}_g \psi(\mathbf{y})} f(\mathbf{y}) d\mathbf{y}$

For $d > 2$, ψ symmetric around $\mathbf{a} \in S^{d-1}$

Orientation Score:

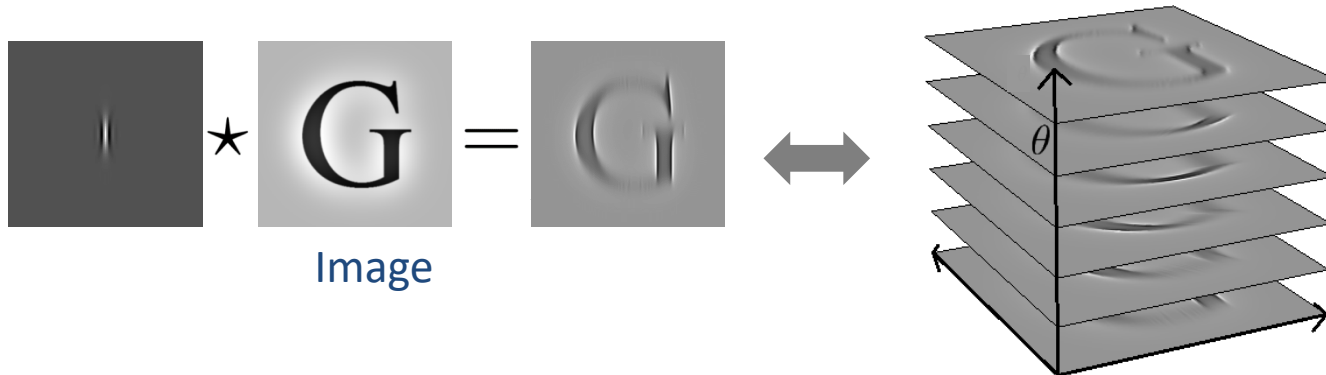
$$\mathbb{R}^d \times S^{d-1} \ni (\mathbf{x}, \mathbf{n}) \mapsto \mathcal{W}_\psi f(\mathbf{x}, \mathbf{n}) = \widetilde{\mathcal{W}}_\psi f(\mathbf{x}, \mathbf{R}_n)$$

Domain: $\mathbb{M} := \mathbb{R}^d \times S^{d-1} := G/H = \text{SE}(d)/(\{\mathbf{0}\} \times SO(d-1))$

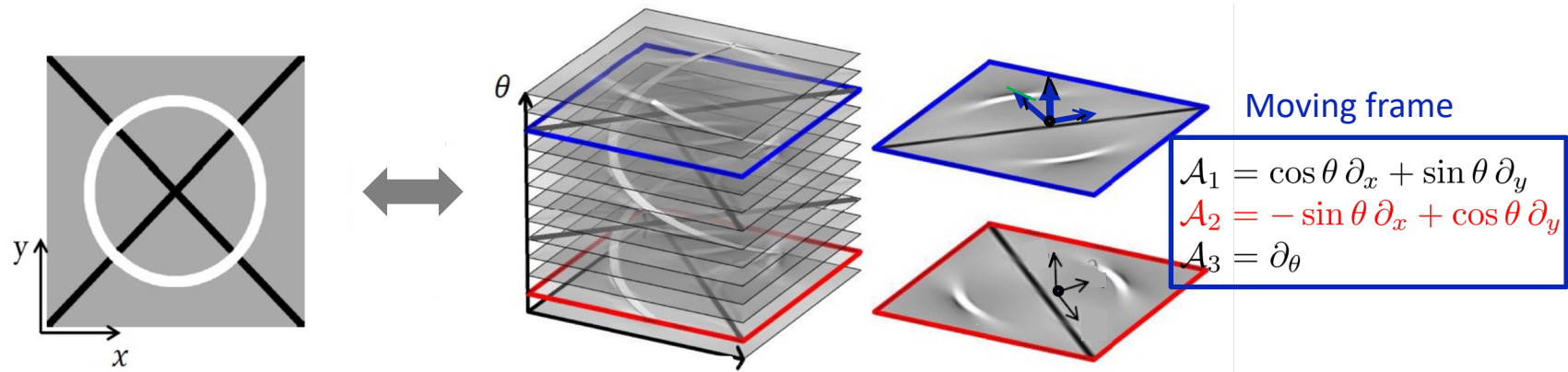
i.e. identify $(\mathbf{x}, \mathbf{n}) \leftrightarrow (\mathbf{x}, \mathbf{R}_n)$ with \mathbf{R}_n any rotation mapping \mathbf{a} to orientation \mathbf{n}



Invertible Orientation Scores



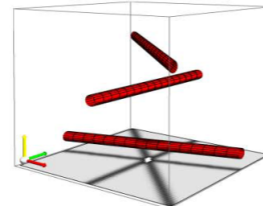
Curved Geometry of $SE(2)$ visible in Score:



In the Orientation Score crossings structures are disentangled:



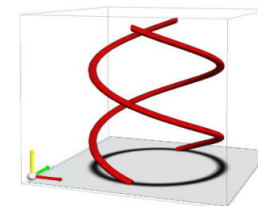
Image



OS

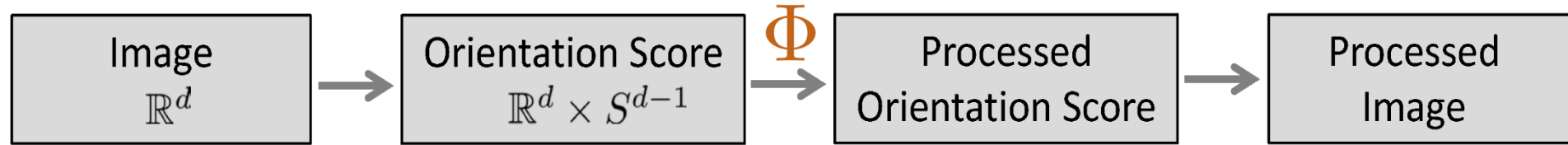


Image

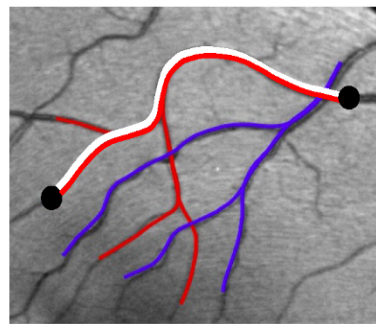
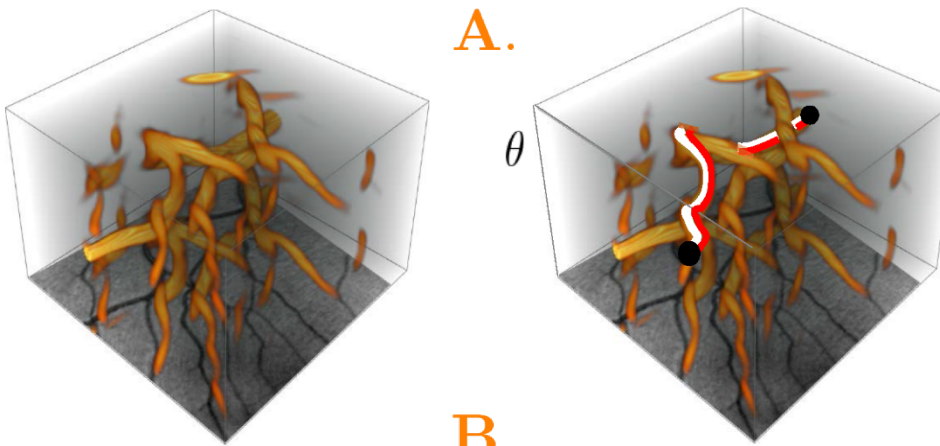


OS

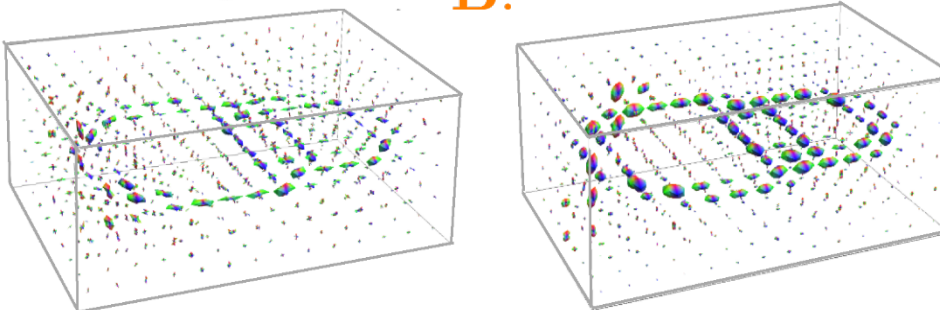
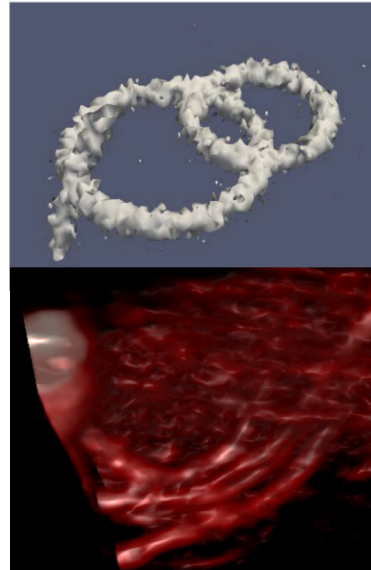
Image Analysis via Invertible Scores



$d = 2$. Tracking Task.

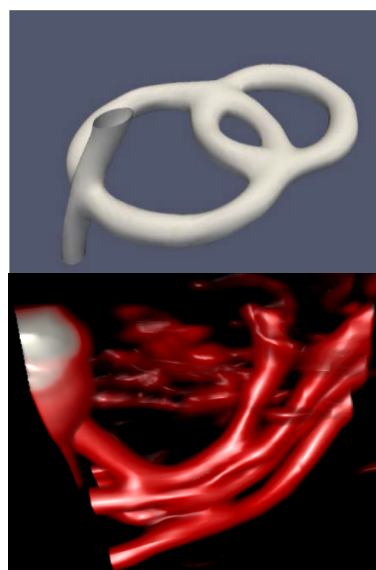


$d = 3$. Task:



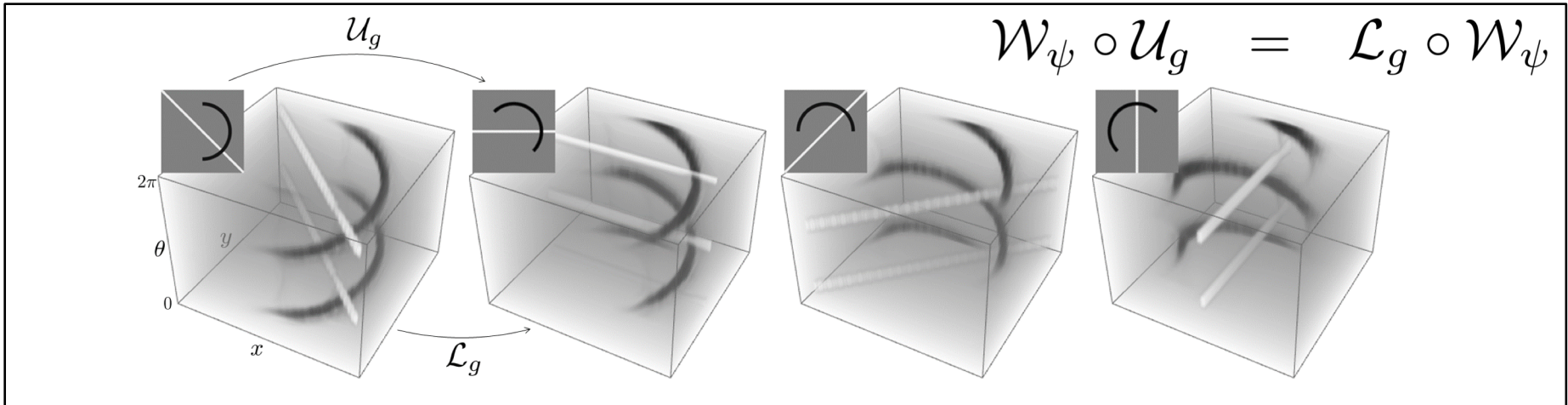
A. Tracking via Optimal Geodesics

B. Enhancement via PDE-flows:
Diffusion, MC or TV
on $\mathbb{M} = \mathbb{R}^d \rtimes S^{d-1}$

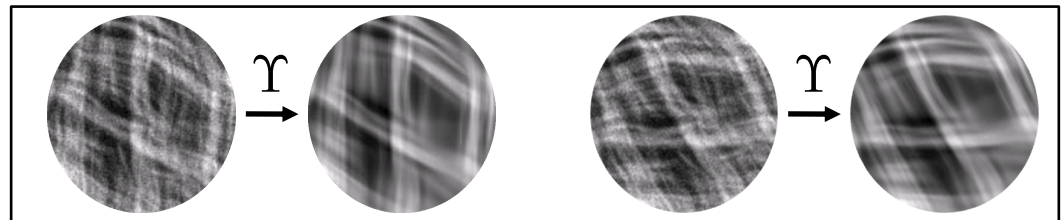


Left-invariant processing on the score

Recall $\mathcal{L}_g U(h) = U(g^{-1}h)$ and $\mathcal{R}_g U(h) = U(hg)$.



$$\Upsilon = \mathcal{W}_\psi^* \circ \Phi \circ \mathcal{W}_\psi :$$



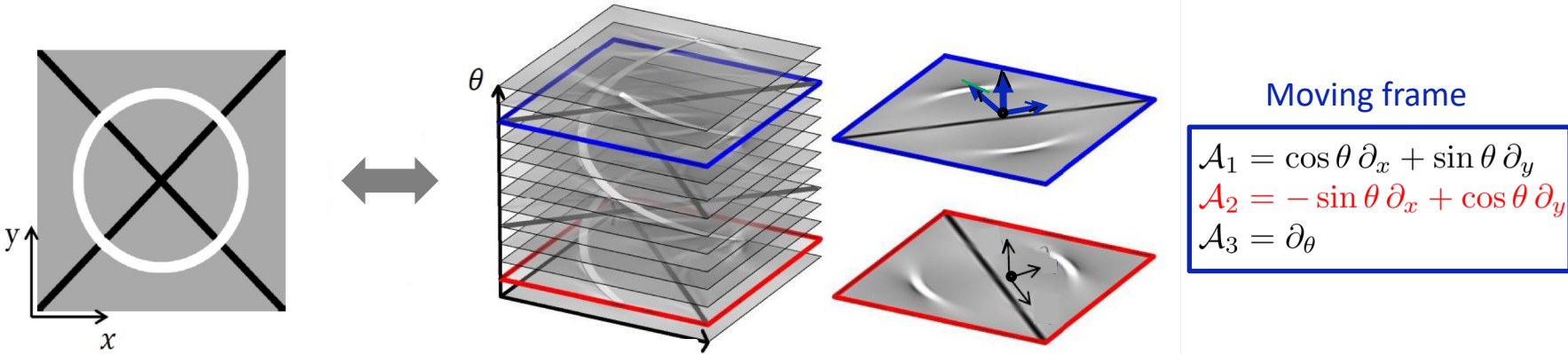
$$\Phi \circ \mathcal{L}_g = \mathcal{L}_g \circ \Phi$$

$$\Phi \circ \mathcal{R}_g \neq \mathcal{R}_g \circ \Phi$$

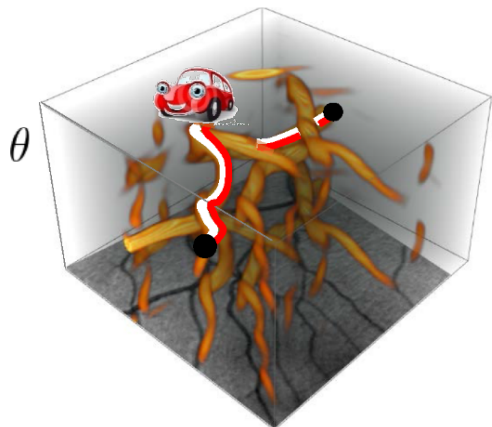
PDE-based image processing by left-invariant vector fields : $\{\mathcal{A}_i\}$

$$\begin{aligned} \mathcal{A}_i|_g &:= (L_g)_*(A_i) = d\mathcal{R}(A_i) \\ A_i &= \mathcal{A}_i|_e \end{aligned}$$

Both by Left-invariant PDEs on \mathbb{M}



PART A. Tracking: Steepest Descent on Wavefronts in score via eikonal PDE



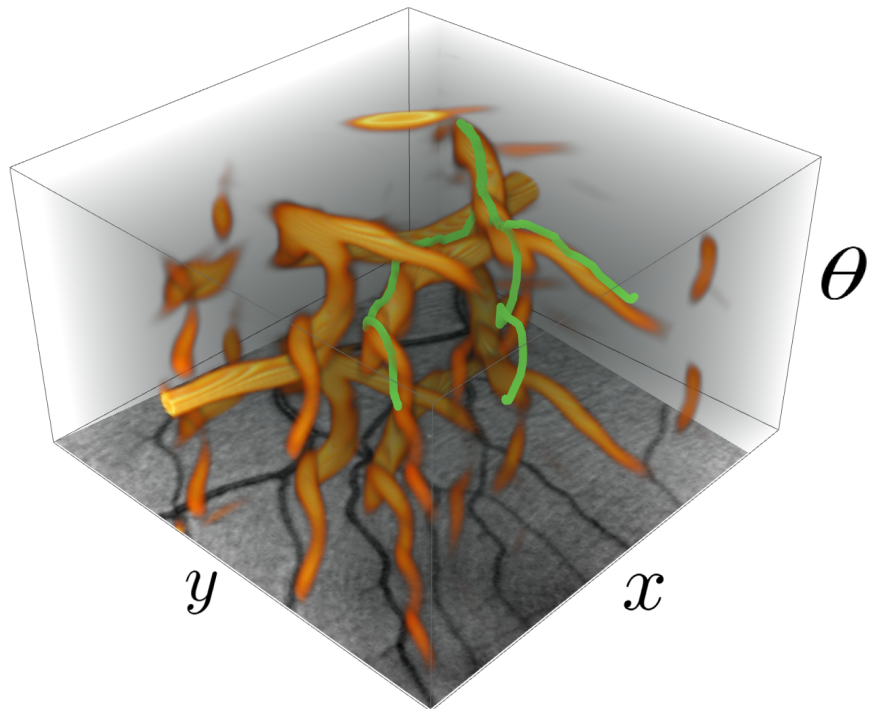
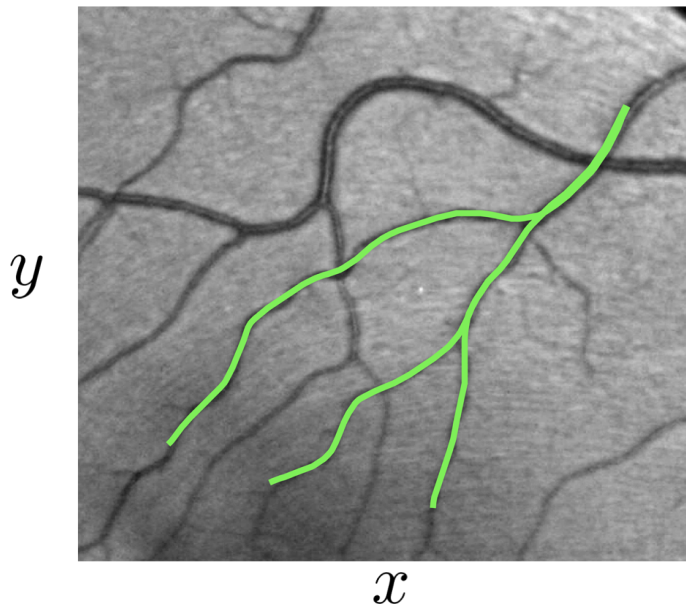
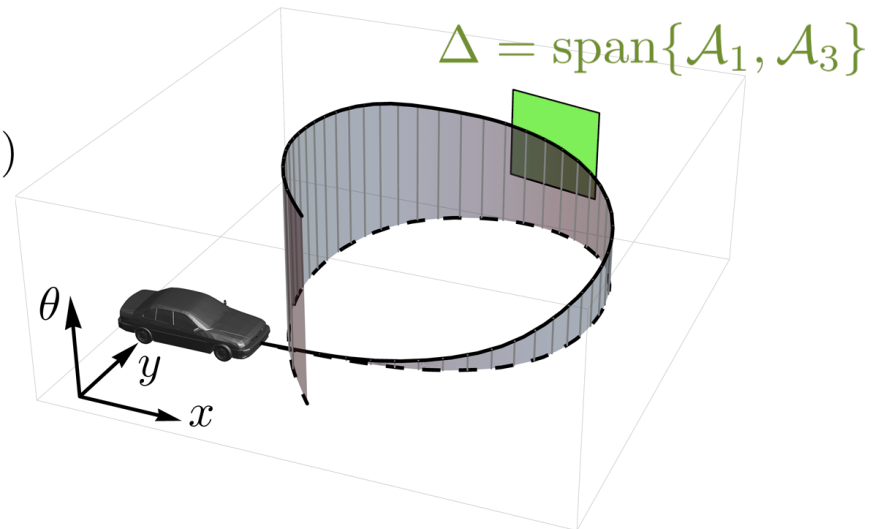
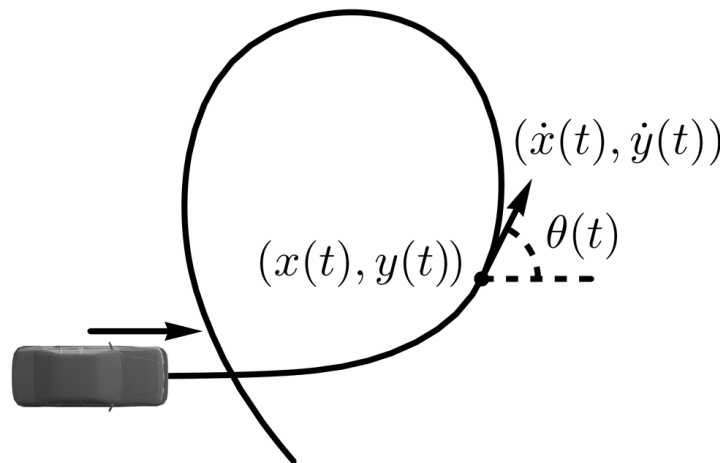
$$\left\{ \begin{array}{l} \sqrt{\sum_{i,j \in \{1,3\}} g^{ij}(g) \mathcal{A}_i W(g) \mathcal{A}_j W(g)} = 1, \quad g = (\mathbf{x}, \mathbf{R}) \in SE(d) \setminus S, \\ U(g) = 0, \quad g \in S \text{ (source set)} \end{array} \right.$$

puts costs on the “car” controls:
 - spatial velocity
 - angular velocity

PART B. Enhancement: Evolutions on score

$$\left\{ \begin{array}{l} \frac{\partial W}{\partial t} = \sum_{i=1}^n -a^i \mathcal{A}_i W + \sum_{i,j=1}^n \mathcal{A}_i (D^{ij} \mathcal{A}_j W) \mp \sum_{i,j=1}^n g^{ij} \mathcal{A}_i W \cdot \mathcal{A}_j W \\ W|_{t=0} = \mathcal{W}_\psi f \end{array} \right.$$

PART A: Tracking via Reeds-Shepp Cars in Orientation Scores

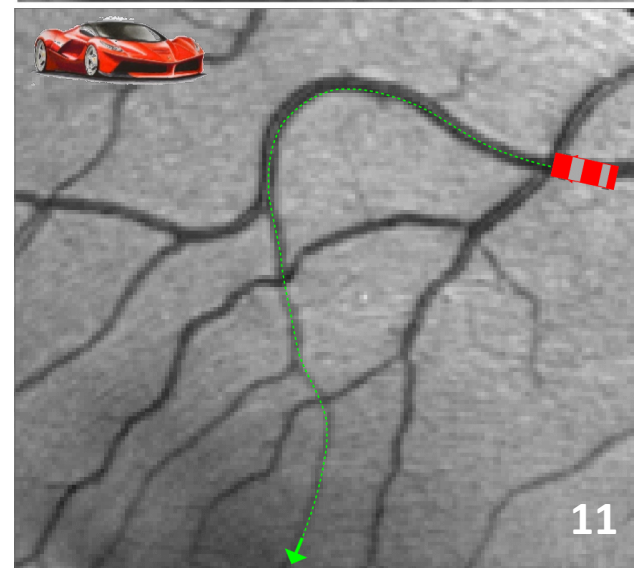
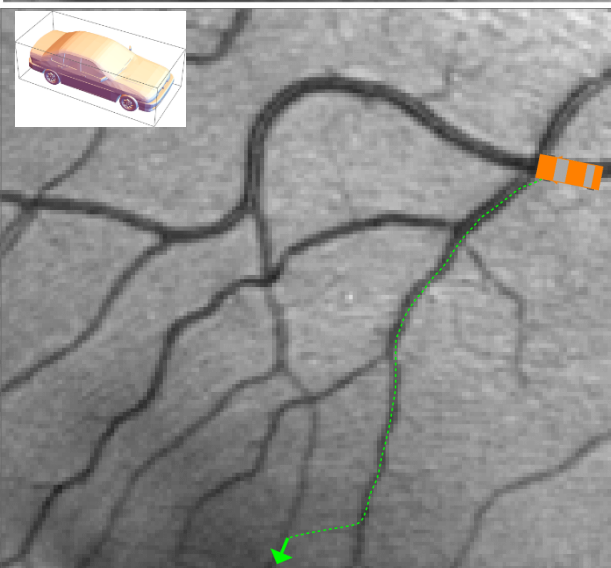
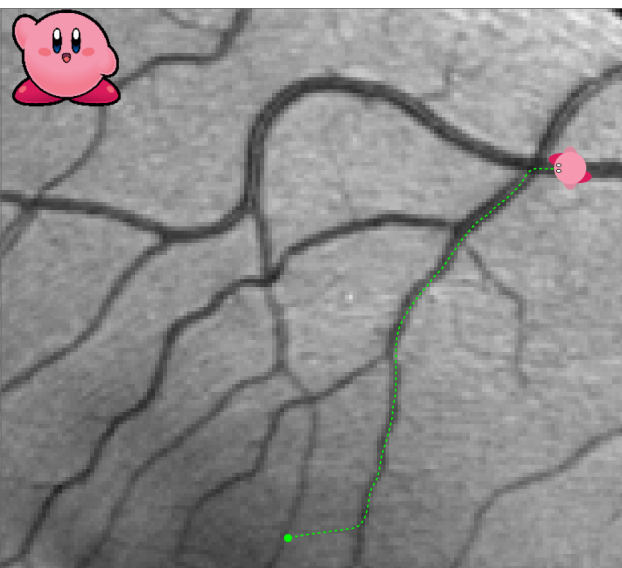
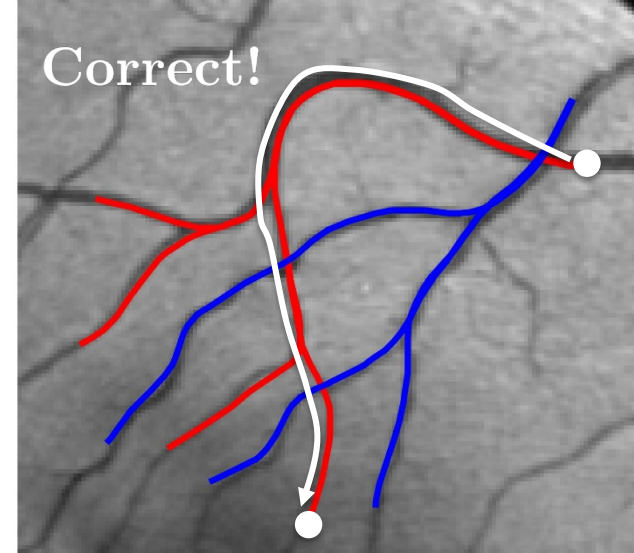
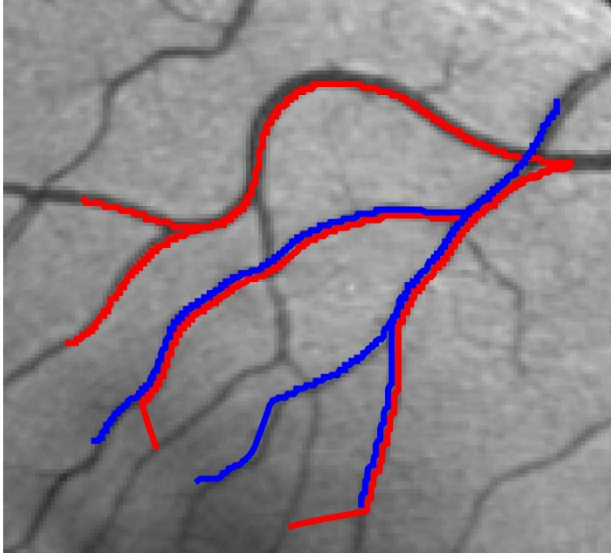
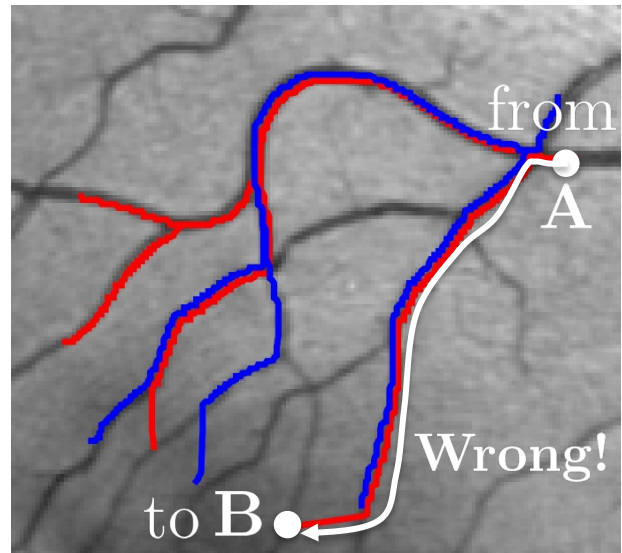


Vessel Tracking

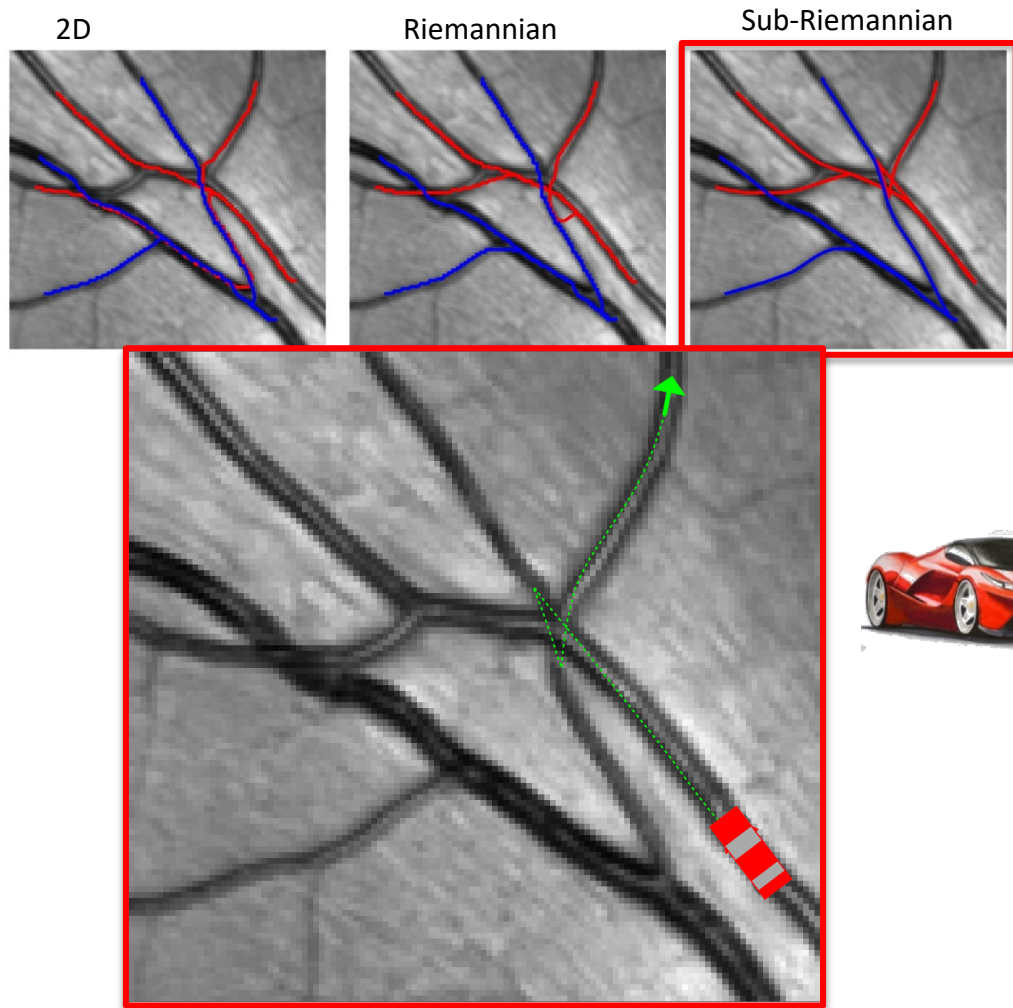
Standard Riemannian
shortest paths in \mathbb{R}^2

Riemannian (Isotropic)
shortest paths in $SE(2)$

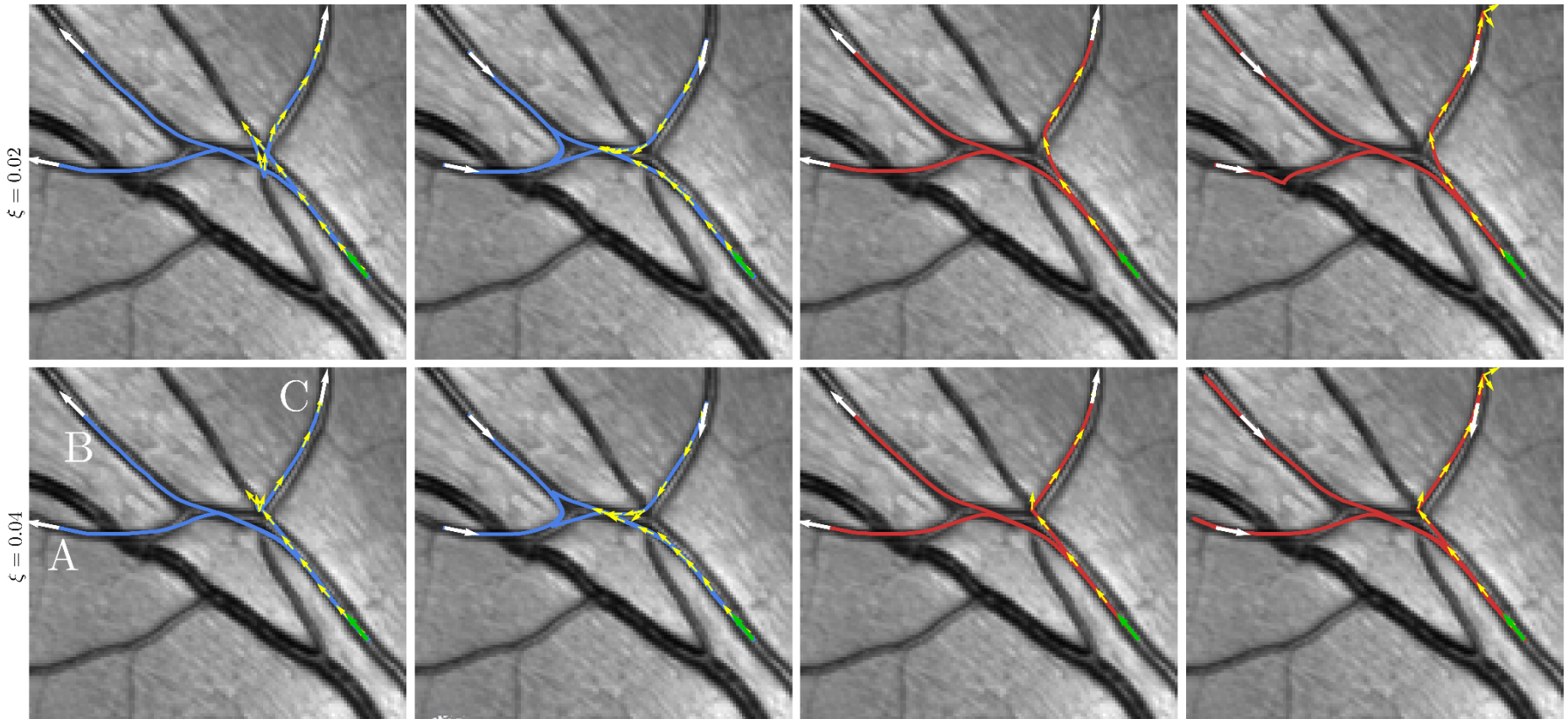
Sub-Riemannian shortest
paths in $SE(2)$



The Cusp Problem: Turn Off the Reverse Gear of the Ferrari..



Sub-Riemannian vs. Asymmetric Finsler Geodesics in Orientation Scores



Bekkers, Duits, Mashtakov, Sanguinetti

SIIMS 2015

Sanguinetti, Bekkers, Duits, Mashtakov, Mirebeau
CIARP 2015



Duits & Meesters & Mirebeau &
Portegies JMIV 2017

Tracking Globally Optimal Geodesics in Orientation Scores

Quasi-distance on \mathbb{M}

$$\mathbf{p} = (\mathbf{x}, \mathbf{n}) \in \mathbb{M}, \\ \mathbf{n} \in S^{d-1}$$

$$d_{\mathcal{F}}(\mathbf{p}_S, \mathbf{p}) = \min_{\substack{\gamma \in \text{Lip}([0, 1], \mathbb{M}), \\ \gamma(0) = \mathbf{p}_S, \gamma(1) = \mathbf{p}}} \int_0^1 \mathcal{F}(\gamma(t), \dot{\gamma}(t)) dt.$$

$$\mathcal{F}(\mathbf{p}, \dot{\mathbf{p}}) = \begin{cases} \mathcal{C}(\mathbf{x}, \mathbf{n}) \sqrt{\xi^2 |(\dot{\mathbf{x}} \cdot \mathbf{n})|^2 + \|\dot{\mathbf{n}}\|^2} & \text{if } \dot{\mathbf{x}} \wedge \mathbf{n} \neq 0 \\ \infty & \text{else} \end{cases}$$

1. PDE:

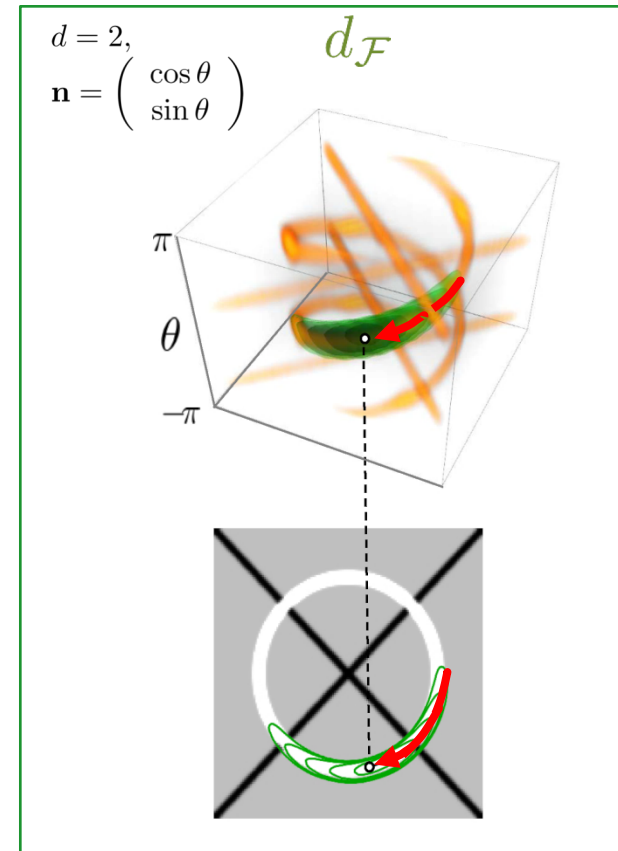
$$\begin{cases} \mathcal{F}^*(dW(\mathbf{p})) = 1, & \mathbf{p} \in \mathbb{M} \setminus S, \\ W(\mathbf{p}) = 0, & \mathbf{p} \in S \end{cases}$$

2. **Viscosity solution** $W(\mathbf{q})$

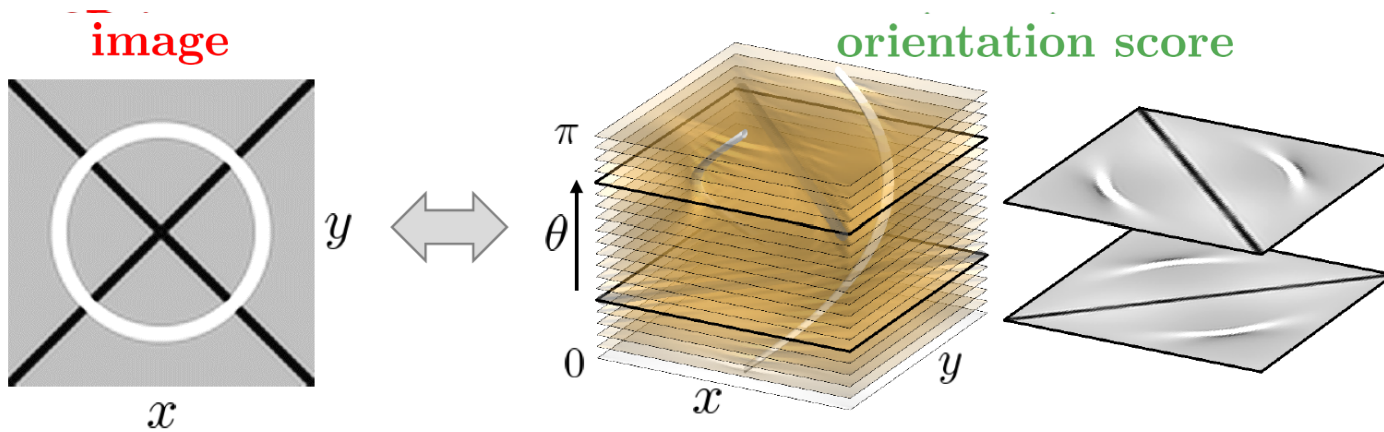
- Anisotropic Fast-Marching Mirebeau 2014
- Iterative PDE method

3. Back-tracking steepest descent

$$\begin{cases} \dot{\gamma}(t) = W(\mathbf{p}) \cdot d_{\hat{\mathbf{p}}} \mathcal{F}^*(\gamma(t), dW(\gamma(t))), \\ \gamma(0) = \mathbf{p}_S, \quad \gamma(1) = \mathbf{p}. \end{cases}$$

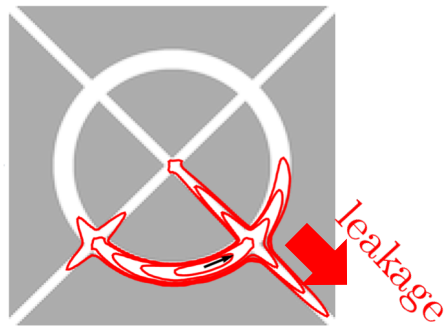


Why track in Orientation Score ?

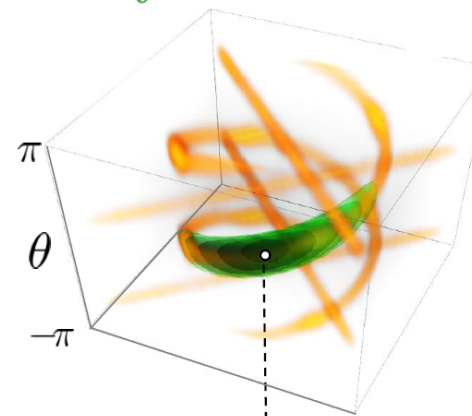


wavefront propagation:
conventional

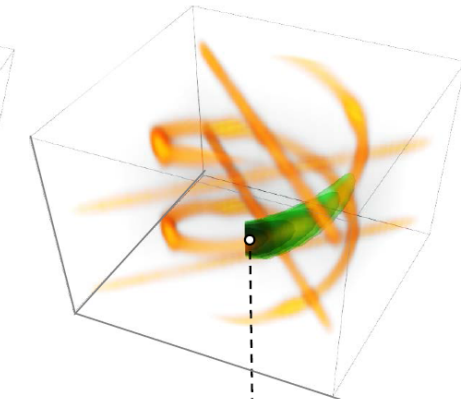
in \mathbb{R}^2
via image



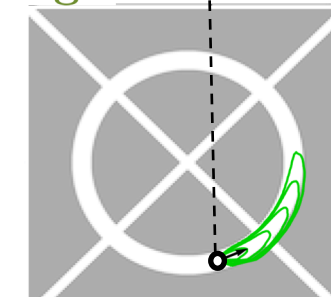
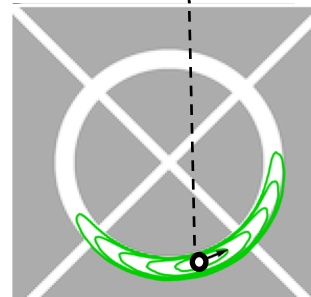
symmetric



asymmetric

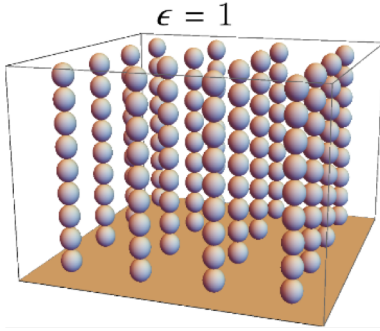


No leakage!

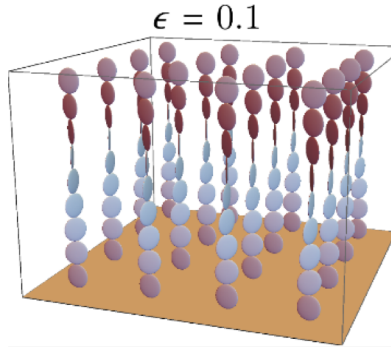


Local Costs for the Reeds-Shepp Car: Finsler Functions \mathcal{F}

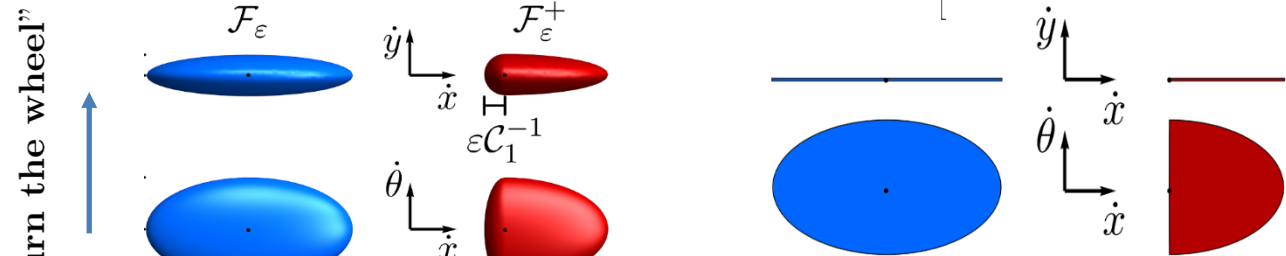
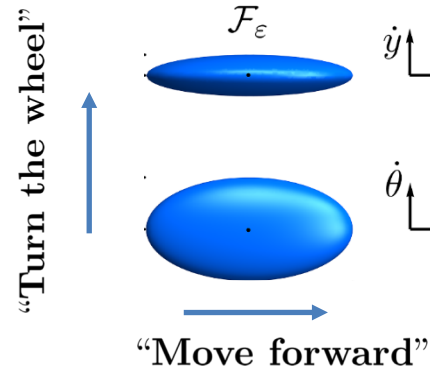
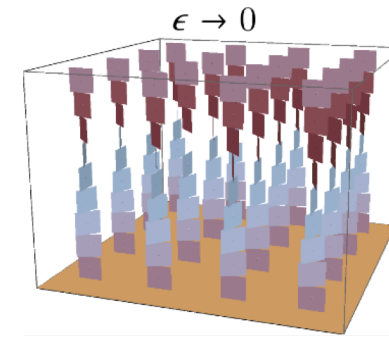
Isotropic Riemannian



Anisotropic Riemannian



Sub-Riemannian



"Turn the wheel"
"Move forward"

$$(\text{(sub)-Riemannian case}) \quad \mathcal{F}(\mathbf{p}, \dot{\mathbf{p}}) = \sqrt{\mathcal{G}|_{\mathbf{p}}(\dot{\mathbf{p}}, \dot{\mathbf{p}})}$$

$$\mathcal{F}_\varepsilon(\mathbf{p}, \dot{\mathbf{p}})^2 := \mathcal{C}_1(\mathbf{p})^2(|\dot{\mathbf{x}} \cdot \mathbf{n}|^2 + \varepsilon^{-2}\|\dot{\mathbf{x}} \wedge \mathbf{n}\|^2) + \mathcal{C}_2(\mathbf{p})^2\|\dot{\mathbf{n}}\|^2,$$

$$\mathcal{F}_0(\mathbf{p}, \dot{\mathbf{p}})^2 := \begin{cases} \mathcal{C}_1^2(\mathbf{p})|\dot{\mathbf{x}} \cdot \mathbf{n}|^2 + \mathcal{C}_2^2(\mathbf{p})\|\dot{\mathbf{n}}\|^2 & \text{if } \dot{\mathbf{x}} \propto \mathbf{n}, \\ +\infty & \text{otherwise.} \end{cases}$$

"Turn off the reverse gear"

$$\mathcal{F}_\varepsilon^+(\mathbf{p}, \dot{\mathbf{p}})^2 := \mathcal{C}_1(\mathbf{p})^2(|\dot{\mathbf{x}} \cdot \mathbf{n}|^2 + \varepsilon^{-2}\|\dot{\mathbf{x}} \wedge \mathbf{n}\|^2 + (\varepsilon^{-2} - 1)(\dot{\mathbf{x}} \cdot \mathbf{n})_-^2) + \mathcal{C}_2(\mathbf{p})^2\|\dot{\mathbf{n}}\|^2$$

$$\mathcal{F}_0(\mathbf{p}, \dot{\mathbf{p}})^2 := \begin{cases} \mathcal{C}_1^2(\mathbf{p})|\dot{\mathbf{x}} \cdot \mathbf{n}|^2 + \mathcal{C}_2^2(\mathbf{p})\|\dot{\mathbf{n}}\|^2 & \text{if } \dot{\mathbf{x}} \propto \mathbf{n}, \text{ and } \dot{\mathbf{x}} \cdot \mathbf{n} \geq 0 \\ +\infty & \text{otherwise.} \end{cases}$$

Eikonal PDE & tracking require Dual Finsler Function \mathcal{F}^*

Finsler function approximations of the Reeds-Shepp car



$$\mathcal{F}_\varepsilon(\mathbf{p}, \dot{\mathbf{p}})^2 := \mathcal{C}_1(\mathbf{p})^2(|\dot{\mathbf{x}} \cdot \mathbf{n}|^2 + \varepsilon^{-2}\|\dot{\mathbf{x}} \wedge \mathbf{n}\|^2) + \mathcal{C}_2(\mathbf{p})^2\|\dot{\mathbf{n}}\|^2,$$



$$\mathcal{F}_\varepsilon^+(\mathbf{p}, \dot{\mathbf{p}})^2$$

Definition

$$\mathcal{F}^*(\mathbf{p}, \hat{\mathbf{p}}) := \sup_{\dot{\mathbf{p}} \in T_{\mathbf{p}}\mathbb{M} \setminus \{0\}} \frac{\langle \hat{\mathbf{p}}, \dot{\mathbf{p}} \rangle}{\mathcal{F}(\mathbf{p}, \dot{\mathbf{p}})}$$

For $\epsilon \downarrow 0$

$$\text{hard-constraint } \dot{\mathbf{x}} = +(\dot{\mathbf{x}} \cdot \mathbf{n}) \cdot \mathbf{n}$$

and eikonal equation:

$$(\mathcal{F}^+)^*(\mathbf{p}, dU(\mathbf{p})) = 1$$

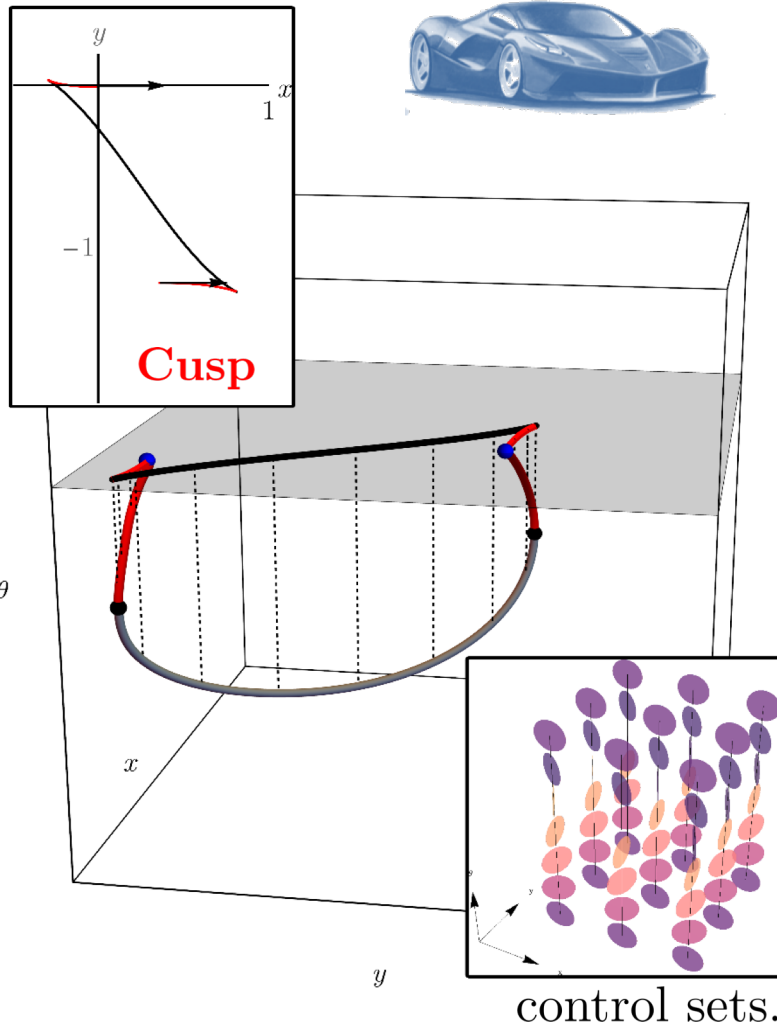
\Leftrightarrow

$$\sqrt{(\mathcal{C}_1(\mathbf{p}))^{-2} \|\nabla_{S^{d-1}} U\|^2 + (\mathcal{C}_2(\mathbf{p}))^{-2} (\mathbf{n} \cdot \nabla_{\mathbb{R}^d} U)_+^2} = 1$$

The Reeds Shepp Car with and without Reverse Gear

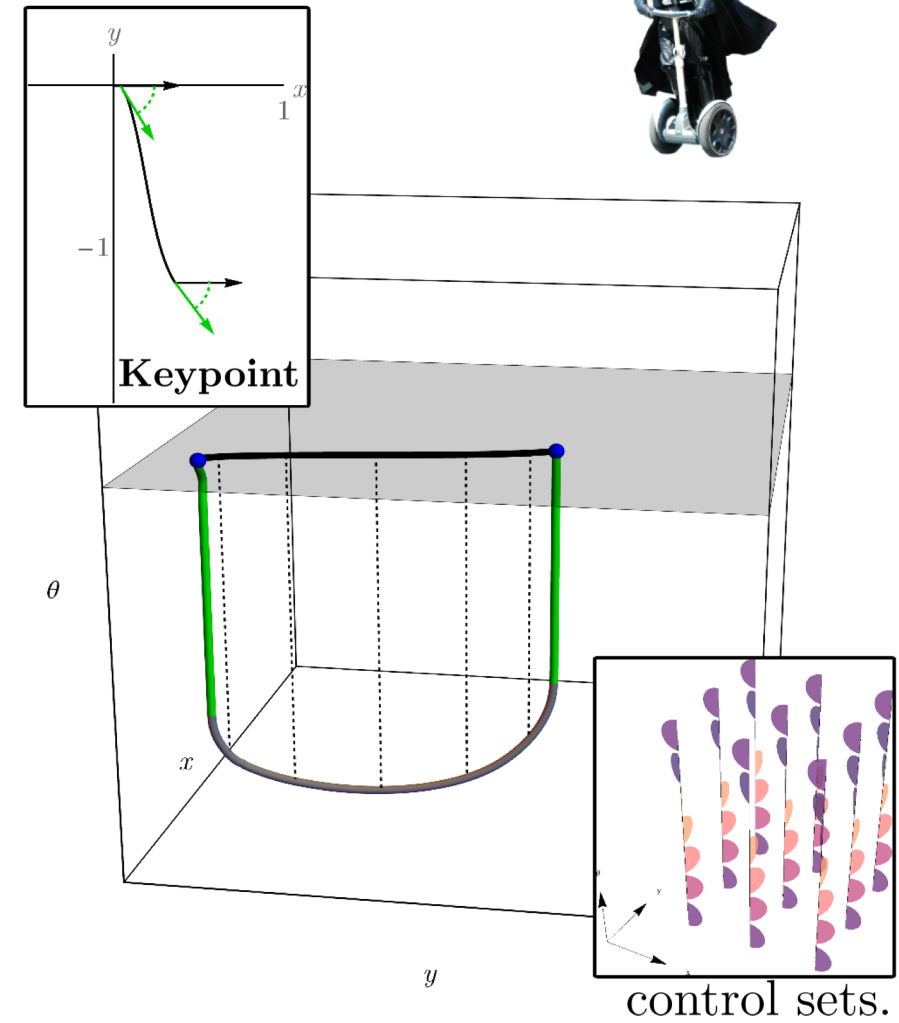
Sub-Riemannian

With reverse gear



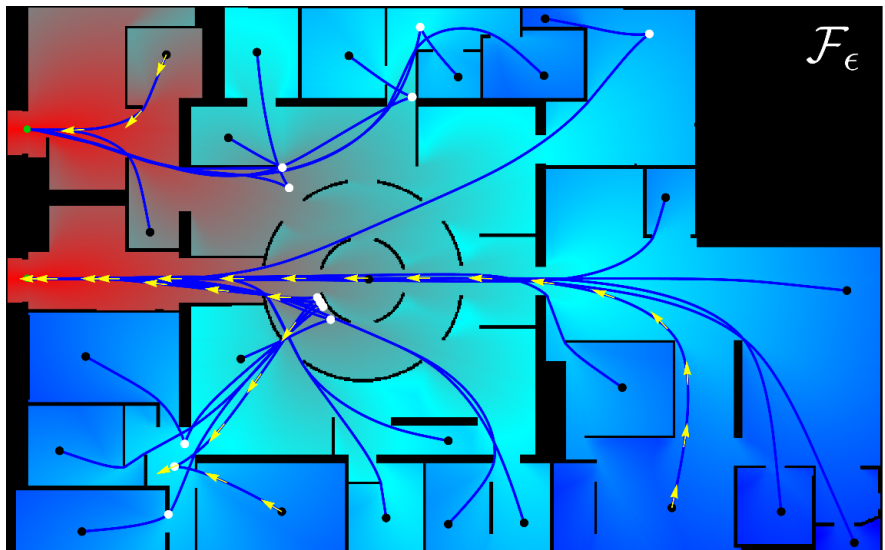
Asymmetric Version

Without reverse gear

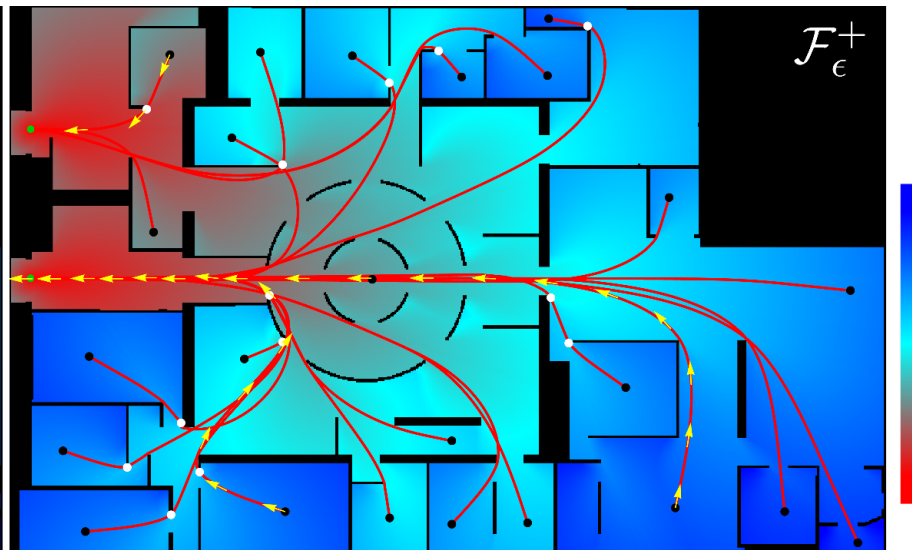


Cusps in Spatially Projected Sub-Riemannian Geodesics or Key-points in Asymmetric Finsler Geodesics?

Sub-Riemannian



Asymmetric Version



4 Fundamental Theorems

On the following topics:

1. (Local) controllability properties,
2. Convergence (of distance and minimizers) when $\epsilon \downarrow 0$,
3. Location of Cusps or Keypoints for uniform costs/mobility,
4. Back-tracking of minimizers by intrinsic gradient, descent

w.r.t. Models $(\mathbb{M}, d_{\mathcal{F}})$ with $\mathcal{F} = \mathcal{F}_\epsilon, \mathcal{F}_\epsilon^+, \mathcal{F}_0, \mathcal{F}_0^+$.

Theorem 1

- Both Models: Minimizers exist and global controllability.
- The Reeds-Shepp model without reverse gear is not locally controllable, since

$$\limsup_{\mathbf{p}' \rightarrow \mathbf{p}} d_{\mathcal{F}_0^+}(\mathbf{p}, \mathbf{p}') \geq 2\pi\delta, \text{ for all } \mathbf{p} \in \mathbb{M}.$$

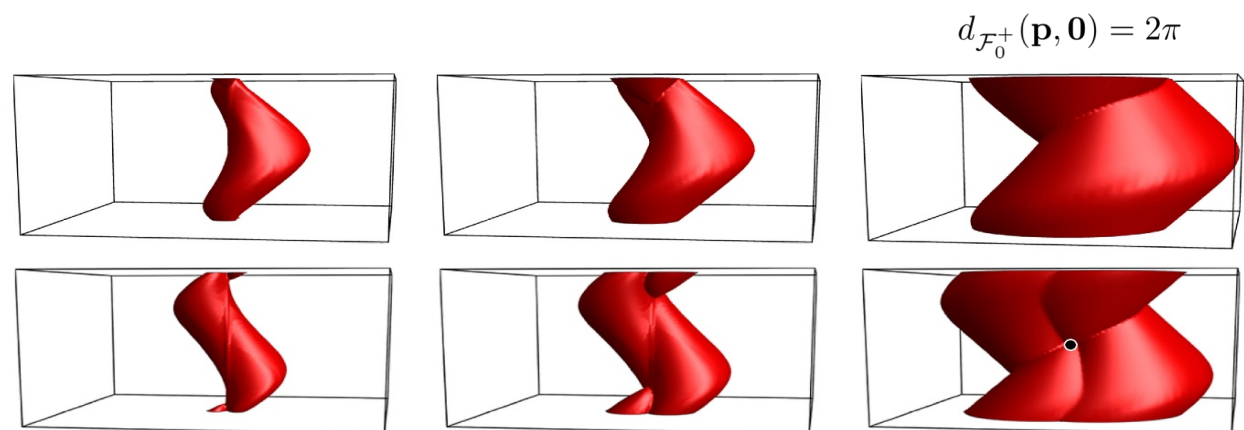
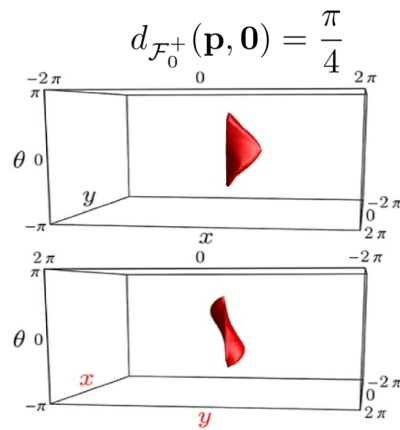
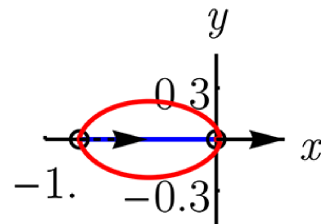
- The sub-Riemannian Reeds-Shepp model is locally controllable, since

$$d_{\mathcal{F}_0}(\mathbf{p}, \mathbf{p}') = \mathcal{O} \left(\mathcal{C}_2(\mathbf{p}) \|\mathbf{n} - \mathbf{n}'\| + \sqrt{\mathcal{C}_2(\mathbf{p}) \mathcal{C}_1(\mathbf{p}) \|\mathbf{x} - \mathbf{x}'\|} \right)$$

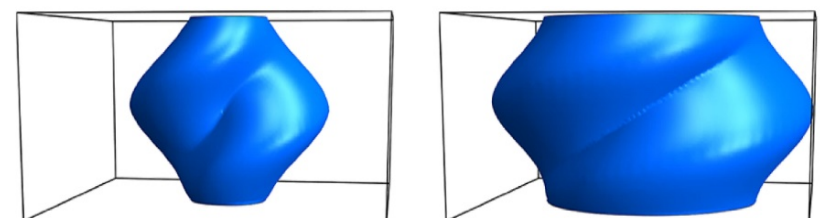
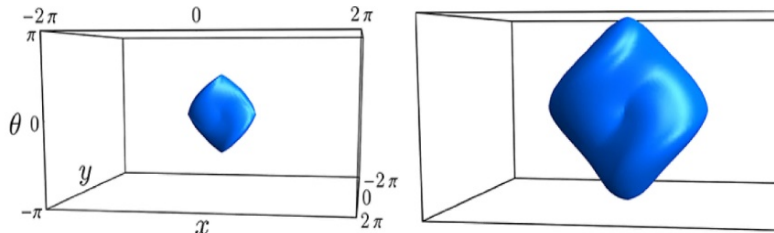
as $\mathbf{p}' = (\mathbf{x}', \mathbf{n}') \rightarrow \mathbf{p} = (\mathbf{x}, \mathbf{n})$.

Illustration Theorem 1

discontinuous
quasi-distance
function $d_{\mathcal{F}_0^+}$



(continuous)
distance
function $d_{\mathcal{F}_0}$



Theorem 2

For all $\mathbf{p}, \mathbf{q} \in \mathbb{M}$:

$$\begin{aligned} d_{\mathcal{F}_\varepsilon}(\mathbf{p}, \mathbf{q}) &\rightarrow d_{\mathcal{F}_0}(\mathbf{p}, \mathbf{q}), & \text{as } \varepsilon \rightarrow 0. \\ d_{\mathcal{F}_\varepsilon^+}(\mathbf{p}, \mathbf{q}) &\rightarrow d_{\mathcal{F}_0^+}(\mathbf{p}, \mathbf{q}), \end{aligned}$$

Consider for each $\varepsilon > 0$ a minimizing path γ_ε^* from \mathbf{p} to \mathbf{q} , with respect to the metric \mathcal{F}_ε , parametrized at constant speed

$$\mathcal{F}_\varepsilon(\gamma_\varepsilon^*(t), \dot{\gamma}_\varepsilon^*(t)) = d_{\mathcal{F}_\varepsilon}(\mathbf{p}, \mathbf{q}), \quad \forall t \in [0, 1].$$

Assume that there is a unique minimal path γ^* from \mathbf{p} to \mathbf{q} with respect to the sub-Riemannian distance $d_{\mathcal{F}_0}$

parametrized at constant speed:

$$\mathcal{F}_0(\gamma^*(t), \dot{\gamma}^*(t)) = d_{\mathcal{F}_0}(\mathbf{p}, \mathbf{q}), \quad \forall t \in [0, 1].$$

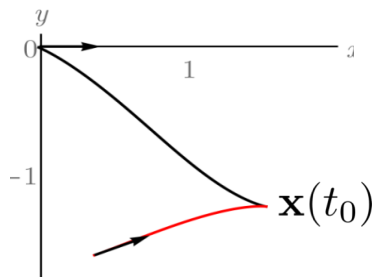
Then $\gamma_\varepsilon^* \rightarrow \gamma^*$ as $\varepsilon \rightarrow 0$, uniformly on $[0, 1]$.

Proof

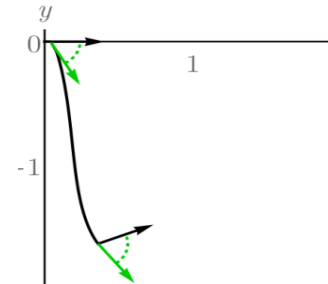
- 1) $d_{\mathcal{F}}(\mathbf{p}, \mathbf{q}) = \inf \{T \geq 0 \mid \exists_{\gamma \in \text{Lip}([0, T], \mathbb{M})} \& \dot{\gamma} \in B_{\mathcal{F}}(\gamma(\cdot))\}$
- 2) closedness of controllable paths
- 3) Arzela-Ascoli
- 4) continuity of controls

Theorem 3

Cusp



Keypoint



Theorem 3 (Cusps and Keypoints) Let $\varepsilon > 0$, $d = 2$, $\mathcal{C}_1 = \mathcal{C}_2 = 1$. Then,

- in $(\mathbb{M}, d_{\mathcal{F}_0})$ cusps are present in spatial projections of almost every optimal SR geodesics when times t are extended on \mathbb{R} until cut-time.
- in $(\mathbb{M}, d_{\mathcal{F}_\varepsilon^+})$ and $(\mathbb{M}, d_{\mathcal{F}_\varepsilon^-})$ and $(\mathbb{M}, d_{\mathcal{F}_0^+})$ no cusps
- in $(\mathbb{M}, d_{\mathcal{F}_\varepsilon^+})$ and $(\mathbb{M}, d_{\mathcal{F}_0})$ and $(\mathbb{M}, d_{\mathcal{F}_\varepsilon^-})$ no keypoints
- in $(\mathbb{M}, d_{\mathcal{F}_0^+})$ keypoints only occur at the endpoints

An optimal geodesic γ_+ in $(\mathbb{M}, d_{\mathcal{F}_0^+})$ from $e = (0, 0, 0)$ to (x, y, θ) has

- no keypoint if $\mathbf{p} \in \overline{\mathfrak{R}}$,
- a keypoint in $(0, 0)$ if $x < 0$,
- a keypoint only in (x, y) if
 - $\mathbf{p} \in \overline{\mathfrak{R}}^c$ and $x \geq 2$,
 - $\mathbf{p} \in \overline{\mathfrak{R}}^c$ and $0 < x < 2$ and $y(x) \leq E(x)$

$$t_{\text{cut}} \geq t_{\text{cusp}}$$

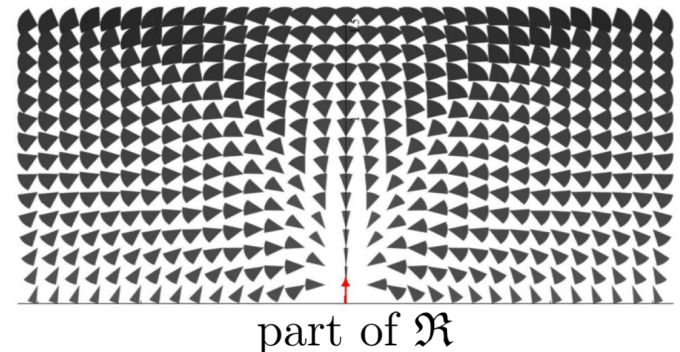
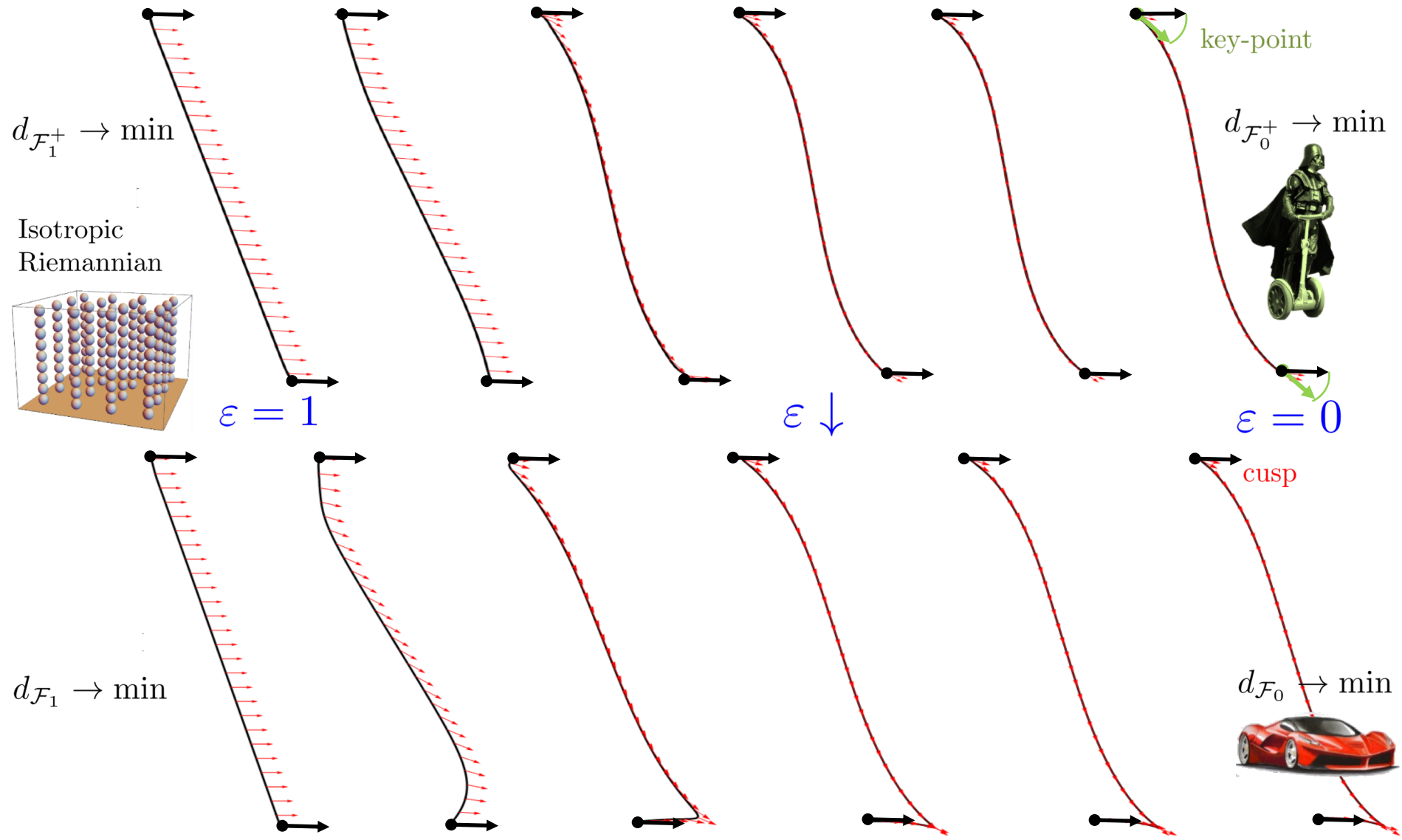


Illustration Theorem 2 & 3



Theorem 4

Theorem 4 (Back-tracking) Let $0 < \varepsilon < 1$. Let $\mathbf{p}_s \in \mathbb{M}$ be a source point. Let $U(\mathbf{p}) := d_{\mathcal{F}_\varepsilon}(\mathbf{p}, \mathbf{p}_s)$, $U^+(\mathbf{p}) := d_{\mathcal{F}_\varepsilon^+}(\mathbf{p}, \mathbf{p}_s)$ be distance maps

For the Riemannian approximation paths of the Reeds-Shepp car we have, provided that U is differentiable at $\gamma(t) = (\mathbf{x}(t), \mathbf{n}(t))$, that

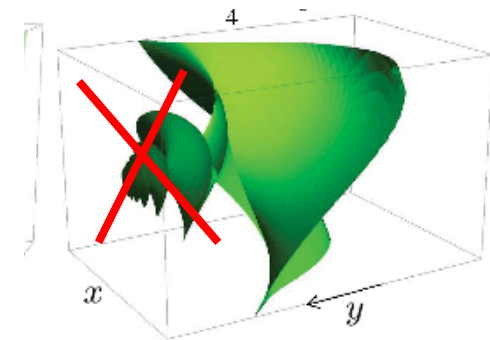
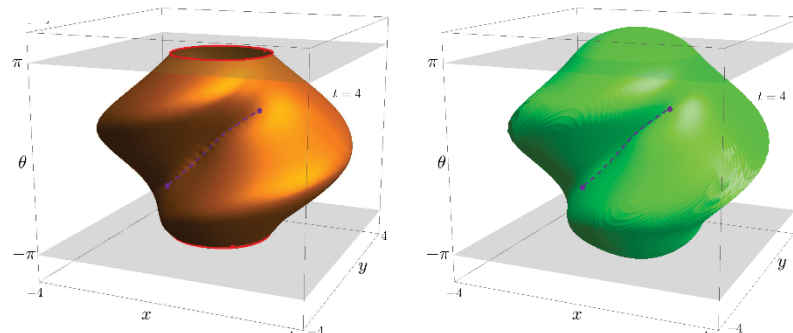
$$\dot{\gamma}(t) = L \mathcal{G}_{\gamma(t); \varepsilon}^{-1} dU(\gamma(t))$$

For the approximation paths of the car without reverse gear we have, provided that U^+ is differentiable at $\gamma^+(t) = (\mathbf{x}^+(t), \mathbf{n}^+(t))$, that

$$\dot{\gamma}^+(t) = L \begin{cases} \mathcal{G}_{\gamma^+(t); \varepsilon}^{-1} dU^+(\gamma^+(t)) & \text{if } \gamma^+(t) \in \mathbb{M}_+ := \{\mathbf{p} \in \mathbb{M} \mid \langle dU^+(\mathbf{p}), \mathbf{n} \rangle > 0\}, \\ \tilde{\mathcal{G}}_{\gamma^+(t); \varepsilon}^{-1} dU^+(\gamma^+(t)) & \text{if } \gamma^+(t) \in \mathbb{M}_-, \end{cases}$$

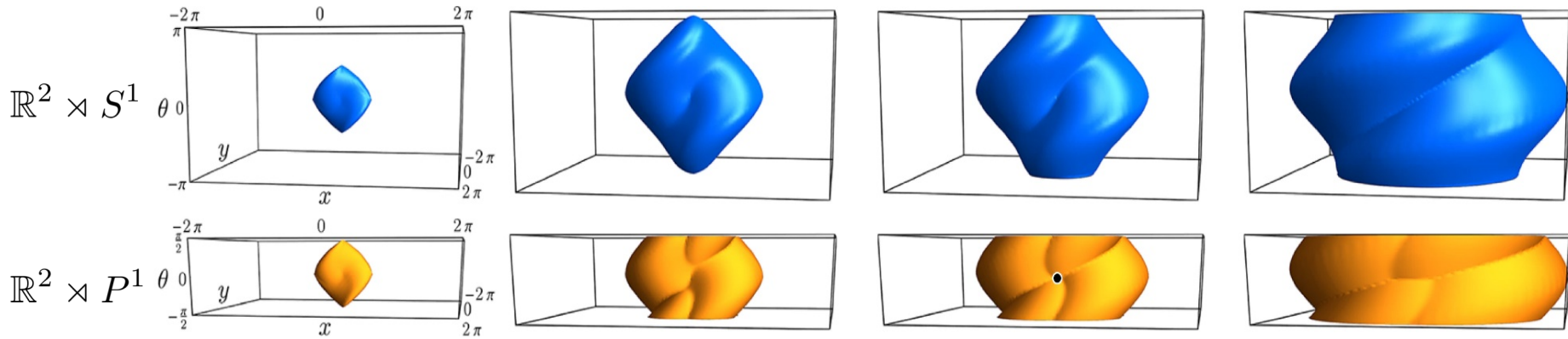
Thm 2 allows limit $\varepsilon \downarrow 0$ to

GLOBAL MINIMIZERS in $(\mathbb{M}, d_{\mathcal{F}_0})$,

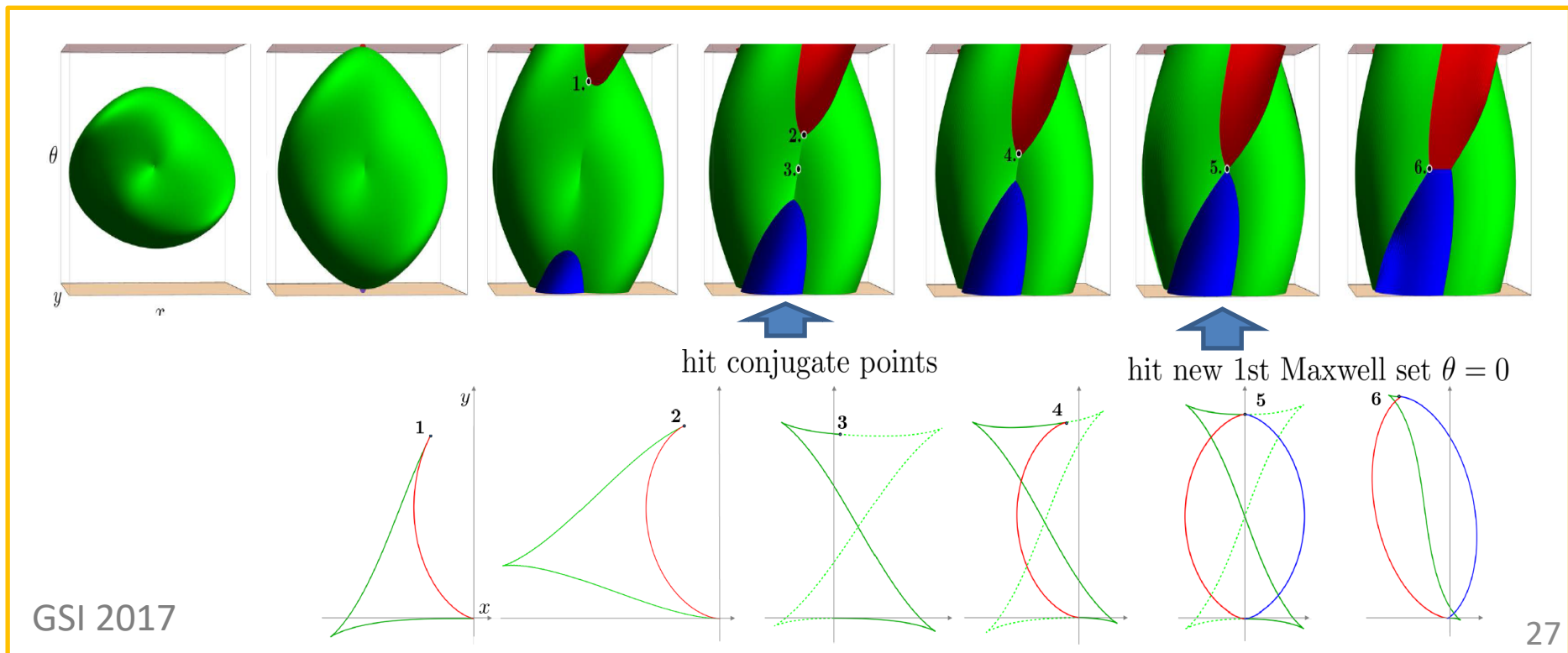


GLOBAL MINIMIZERS IN $(\mathbb{M}, d_{\mathcal{F}_0})$:
concatenations of SR geodesics and spherical geodesics: CORNERS !

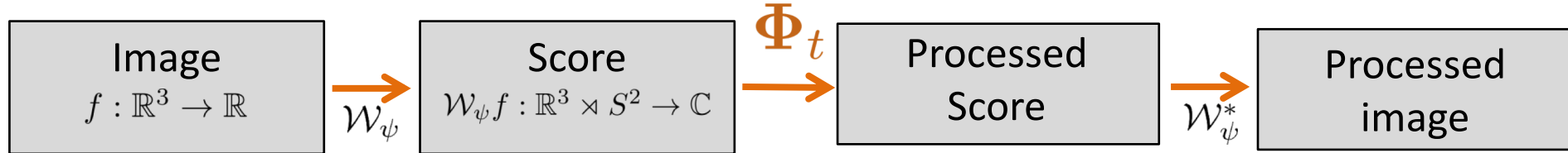
1st Maxwell-set: folds on SR-Spheres



Zoom in in projective line bundle spheres (yellow above):

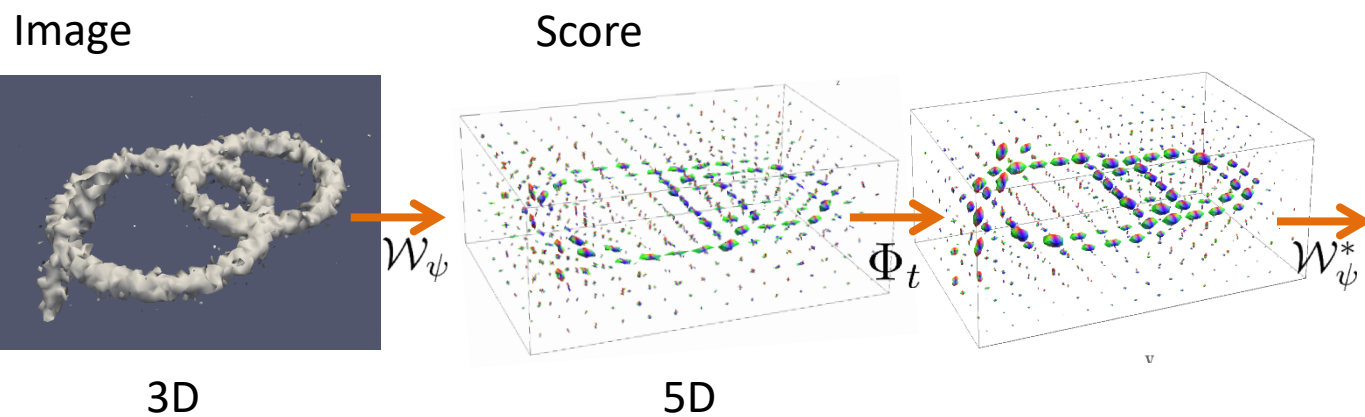
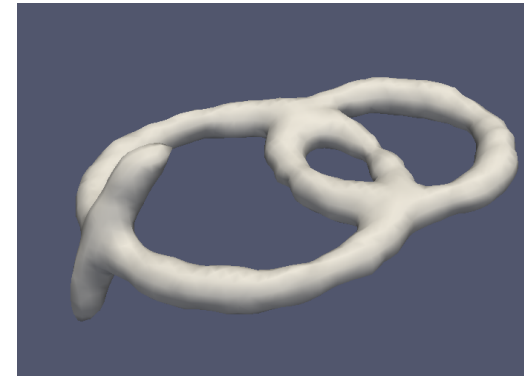


Part B: Enhancement & Denoising via PDEs on \mathbb{M} (Diffusion, TV & MCF Flows)

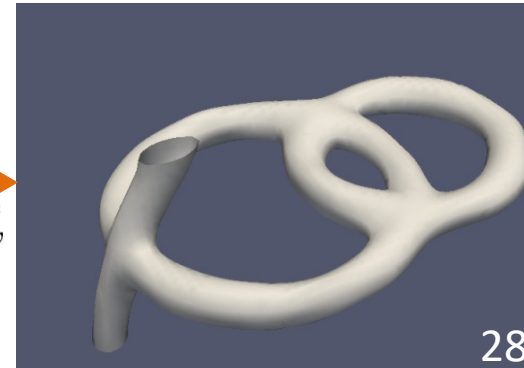


$$\Phi_t : \begin{cases} \frac{\partial \tilde{W}}{\partial t}(\mathbf{x}, \mathbf{R_n}, t) = \sum_{i=1}^5 D_{ii} (\mathcal{B}_i)^2 \tilde{W}(\mathbf{x}, \mathbf{R_n}, t), \\ \tilde{W}(\mathbf{x}, \mathbf{R_n}, 0) = \mathcal{W}_\psi f(\mathbf{x}, \mathbf{n}), \end{cases}$$

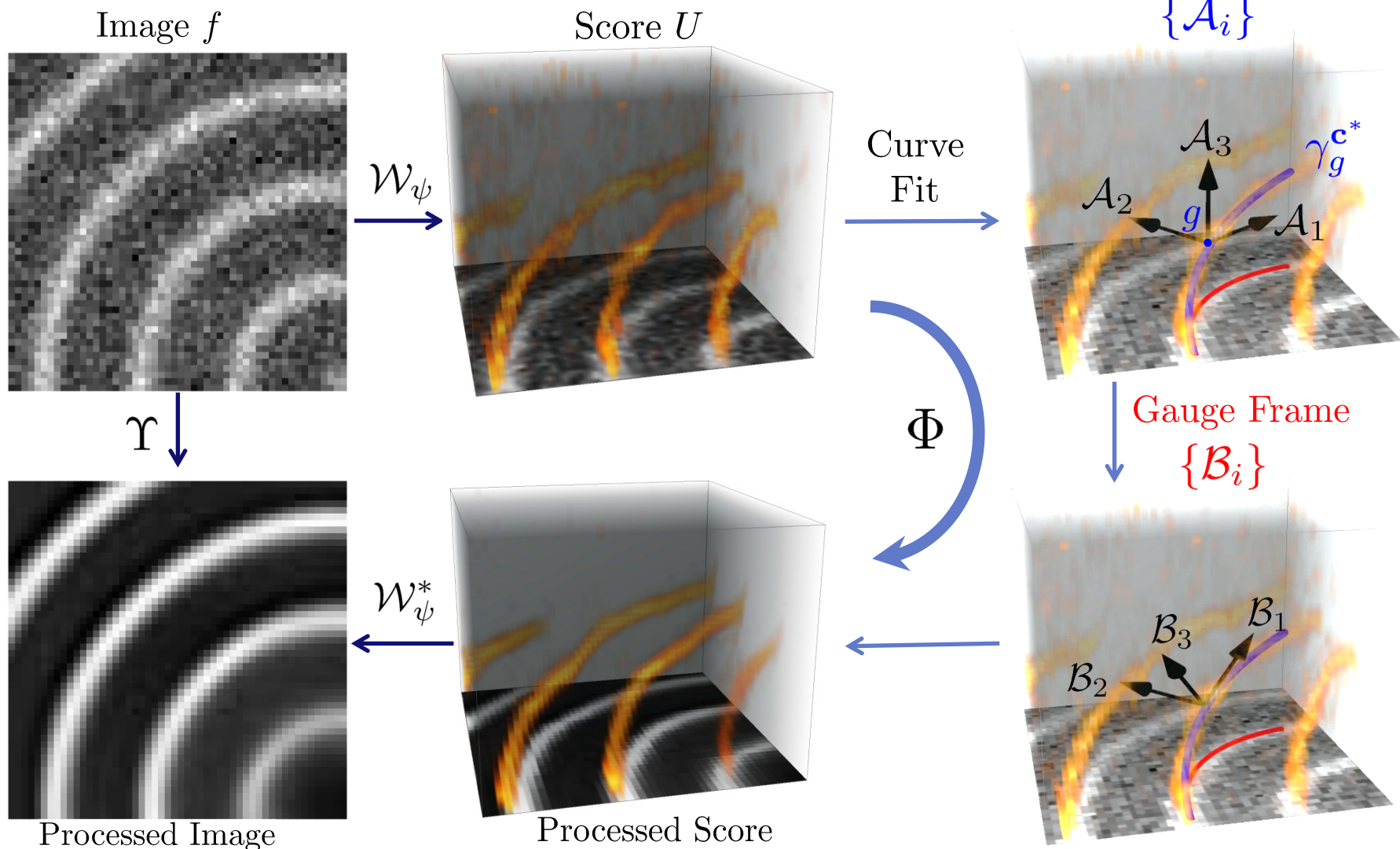
Not adaptive using $\{\mathcal{A}_i\}$



Adaptive using $\{\mathcal{B}_i\}$



Tool of Locally Adaptive Frames



The - Cartan Connection

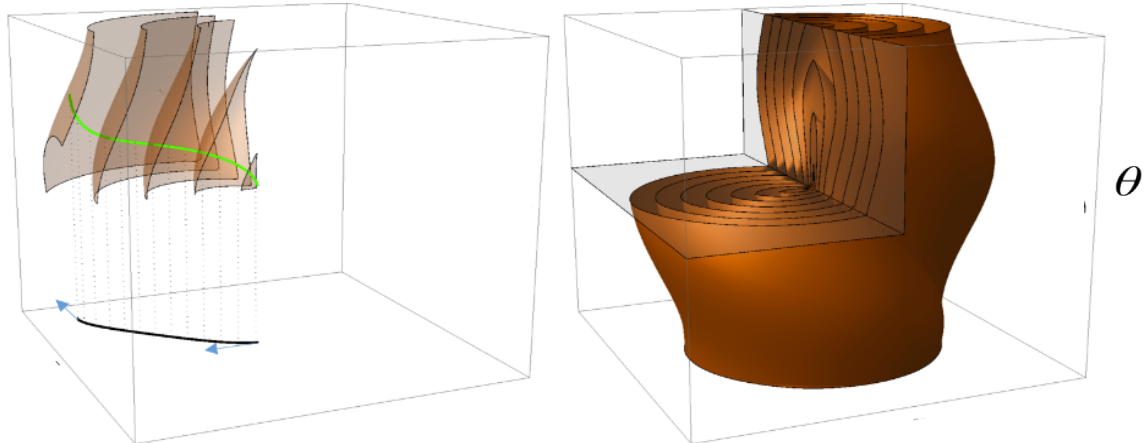
$$\nabla_X \mathcal{A} = \sum_{k=1}^n \left(\dot{a}^k - \sum_{j=1}^n \sum_{i=1}^n c_{i,j}^k a^i \dot{\gamma}^j \right) \mathcal{A}_k \quad \text{for all } X = \sum_{j=1}^n \dot{\gamma}^j \mathcal{A}_j \text{ and } \mathcal{A} = \sum_{k=1}^n a^k \mathcal{A}_k.$$

$$\nabla_X^* \lambda = \sum_{i=1}^n \left(\dot{\lambda}_i + \sum_{j=1}^n \sum_{k=1}^n c_{i,j}^k \lambda_k \dot{\gamma}^j \right) \omega^i.$$

Theorem (Duits NMVis. 2013, JDCCS 2016)

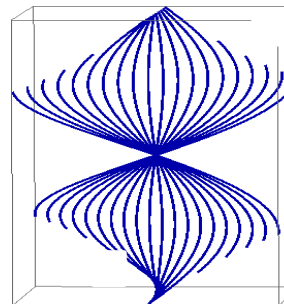
Shortest curves have parallel momentum w.r.t.
partial dual left-Cartan connection, they are *(Sub-)Riemannian geodesics*.

$$\begin{cases} \nabla_{\dot{\gamma}}^* \lambda = 0 \\ \dot{\gamma} = \mathcal{G}^{-1} P_{\Delta^*} \lambda \end{cases}$$



Straight curves have parallel velocity, they are *(horizontal) exponential curves*.

$$\nabla_{\dot{\gamma}} \dot{\gamma} = 0 \text{ and } \dot{\gamma} \in \Delta$$

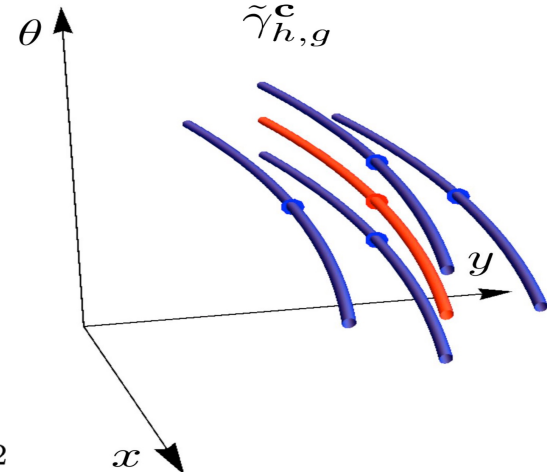


“Straight” Curve Fit Theory in $SE(d)$

Smooth Data

$$U : SE(d) \rightarrow \mathbb{R}$$

$$V := G_s * U$$



Exponential Curve Fits (1st Order)

$$\mathbf{c}^*(g) = \underset{\mathbf{c} \in \mathbb{R}^{m_d}, \|\mathbf{c}\|=1}{\operatorname{argmin}} \int_{SE(d)} G_\rho(h^{-1}g) \left| \frac{d}{dt} V(\tilde{\gamma}_{h,g}^c(t)) \right|_{t=0}^2 dh,$$

Thm. *Solution: e.v. with smallest eigenvalue of a **structure tensor**.*

Exponential Curve Fits (2nd Order)

$$\mathbf{c}^*(g) = \underset{\mathbf{c} \in \mathbb{R}^{m_d}, \|\mathbf{c}\|=1}{\operatorname{argmin}} \left| \frac{d^2}{dt^2} V(\tilde{\gamma}_g^c(t)) \right|_{t=0}, \quad [H(V)]_{ij} \stackrel{\text{def}}{=} (\nabla_{\mathcal{A}_i}^* dV)$$

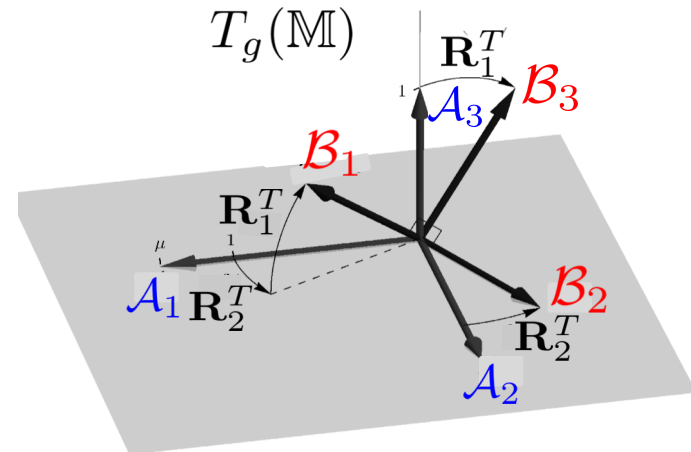
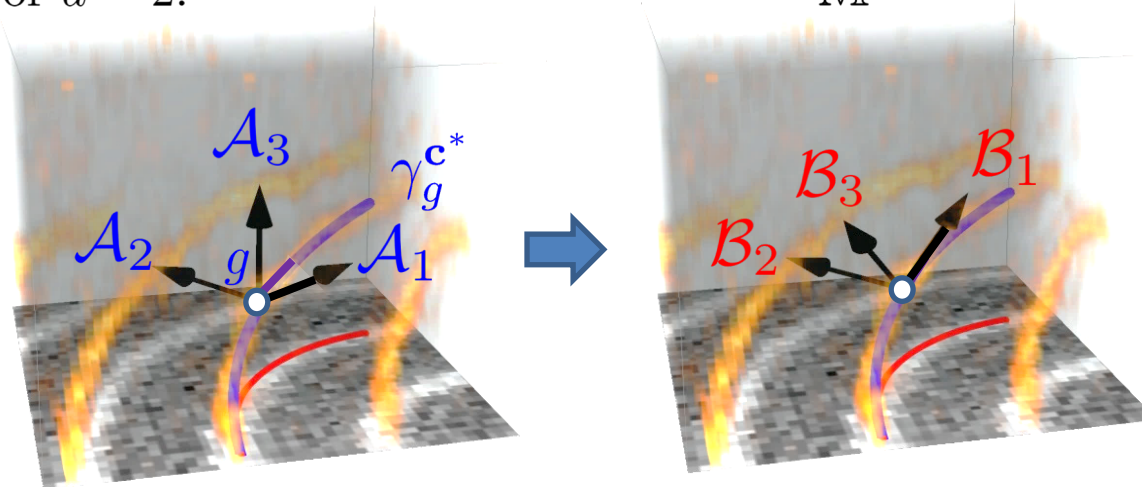
Thm. *If convex then solution: e.v. with smallest abs. ev. of symmetric sum **Hessian**.*

$$\mathbf{c}^*(g) = \underset{\mathbf{c} \in \mathbb{R}^{m_d}, \|\mathbf{c}\|_\mu=1}{\operatorname{argmin}} \int_{SE(d)} G_\rho(h^{-1}g) \cdot \left\| \frac{d}{dt} \nabla V(\tilde{\gamma}_{h,g}^c(t)) \right\|_{t=0}^2 dh.$$

Thm. *Solution: e.v. with smallest ev. of symmetric product **Hessian**.*

From Exp Curve Fit to Frame in SE(d)

For $d = 2$.



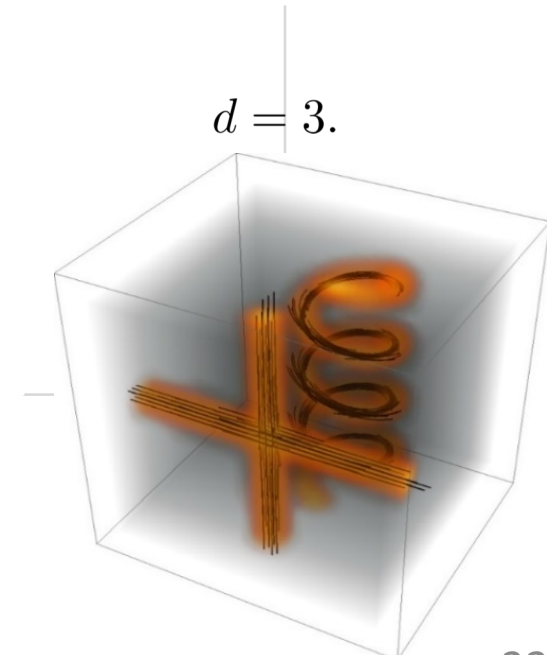
For $d \geq 2$:

$$\underline{\mathcal{A}}|_g \mapsto \underline{\mathcal{B}}|_g := (\mathbf{R}^{\mathbf{c}(g)})^T \mathbf{M}_\mu^{-1} \underline{\mathcal{A}}|_g,$$

with $\mathbf{R}^{\mathbf{c}} = \mathbf{R}_2 \mathbf{R}_1 \in SO(n_d)$, and *planar* rotations $\mathbf{R}_1, \mathbf{R}_2$ s.t.

$$\begin{pmatrix} \mathbf{a} \\ \mathbf{0} \end{pmatrix} \xrightarrow{\mathbf{R}_1} \begin{pmatrix} \mu \|\mathbf{c}^{(1)}\| \mathbf{a} \\ \mathbf{c}^{(2)} \end{pmatrix} \xrightarrow{\mathbf{R}_2} \begin{pmatrix} \mu \mathbf{c}^{(1)} \\ \mathbf{c}^{(2)} \end{pmatrix} = \mathbf{M}_\mu \mathbf{c}.$$

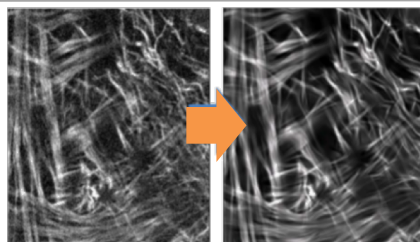
$d = 3$.



Diffusion & Brownian Motions in SE(d)

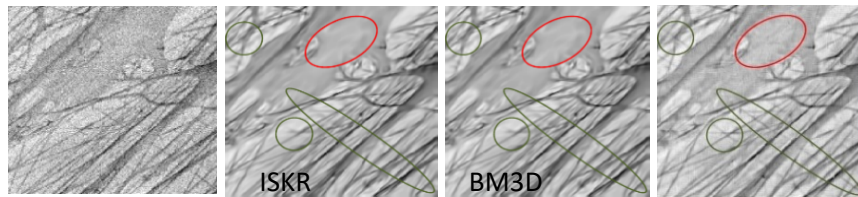
Numerics: Nonlinear Diffusions

2010 IJCV



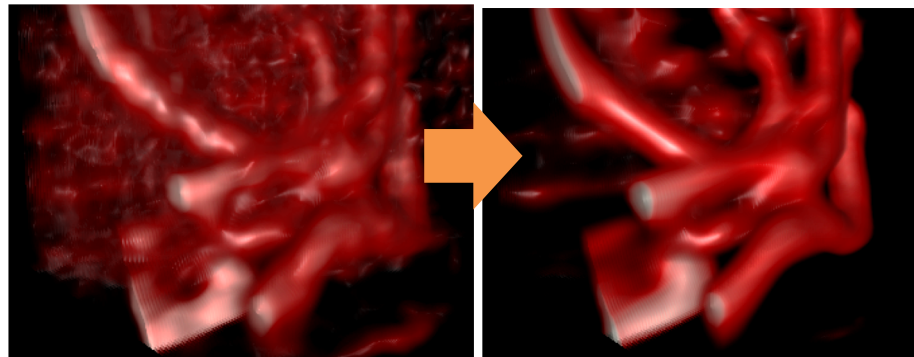
$d = 2$:

2015 ACHA



2018 JMIV

$$d = 3: \quad \begin{cases} \frac{\partial \tilde{W}}{\partial t}(\mathbf{x}, \mathbf{R_n}, t) = \left(\sum_{i=1}^6 D_{ii} (\mathcal{B}_i)^2 \right) \tilde{W}(\mathbf{x}, \mathbf{R_n}, t) \\ \tilde{W}(\mathbf{x}, \mathbf{R_n}, 0) = U(\mathbf{x}, \mathbf{n}) \end{cases}$$

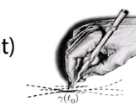


Exact: Linear (convection-)diffusion, α -Stable Lévy

2008 QAM-AMS

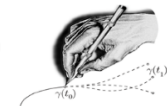
Diffusion
(Contour enhancement)

SE(2)



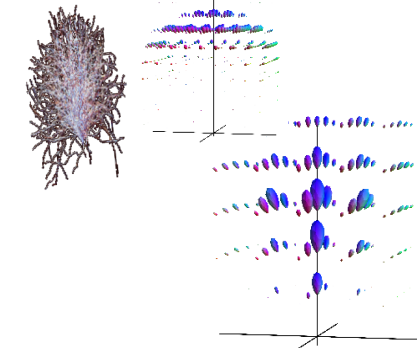
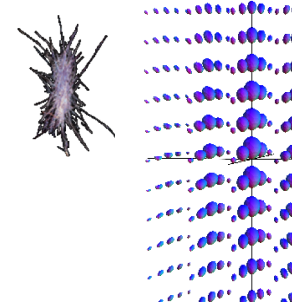
2005 QAM-AMS

Convection-diffusion
(Contour completion)



2016 DGA 2018 Entropy

$$\begin{cases} \frac{\partial \tilde{W}}{\partial t}(\mathbf{x}, \mathbf{R_n}, t) = \left(-a_3 \mathcal{A}_3 + \sum_{i=1}^6 D_{ii} (\mathcal{A}_i)^2 \right) \tilde{W}(\mathbf{x}, \mathbf{R_n}, t) \\ \tilde{W}(\mathbf{x}, \mathbf{R_n}, 0) = U(\mathbf{x}, \mathbf{n}) \end{cases}$$



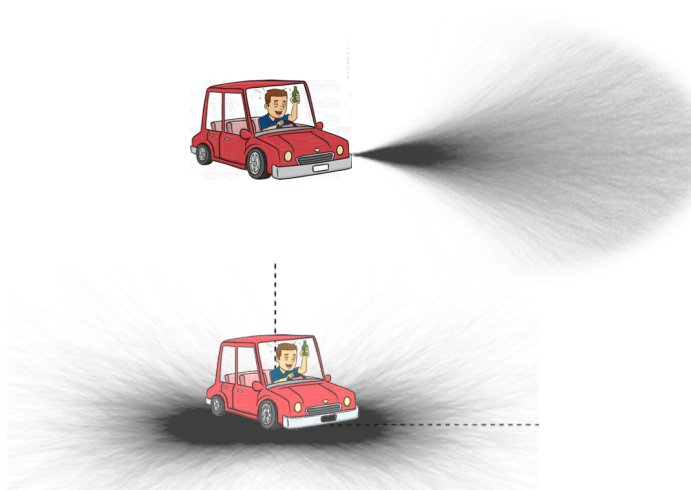
Brownian Motions in $\mathbb{M} = SE(d)/H$

The Drunk Man's.....

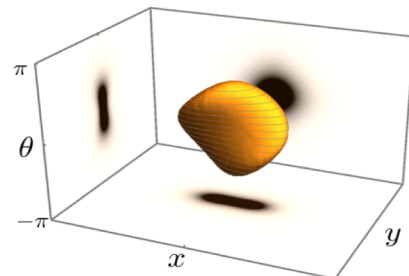
Walk



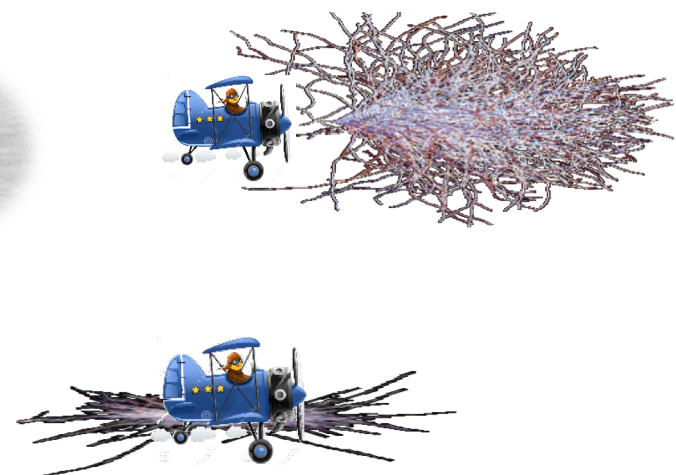
Drive



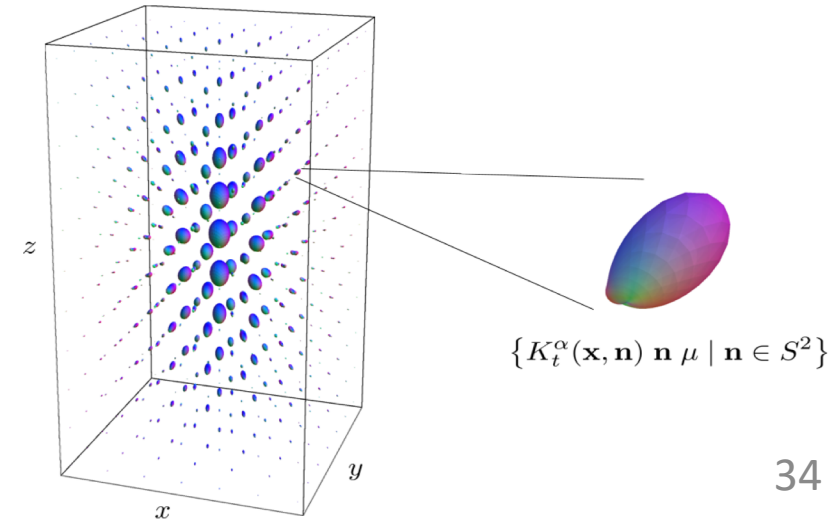
Probability kernel for arriving at
 $(\mathbf{x}, \theta) \in \mathbb{R}^2 \times S^1$ with traveling time t



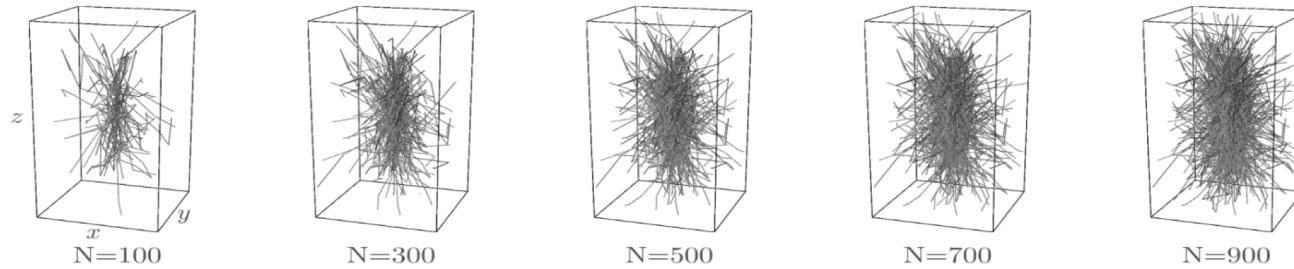
Flight



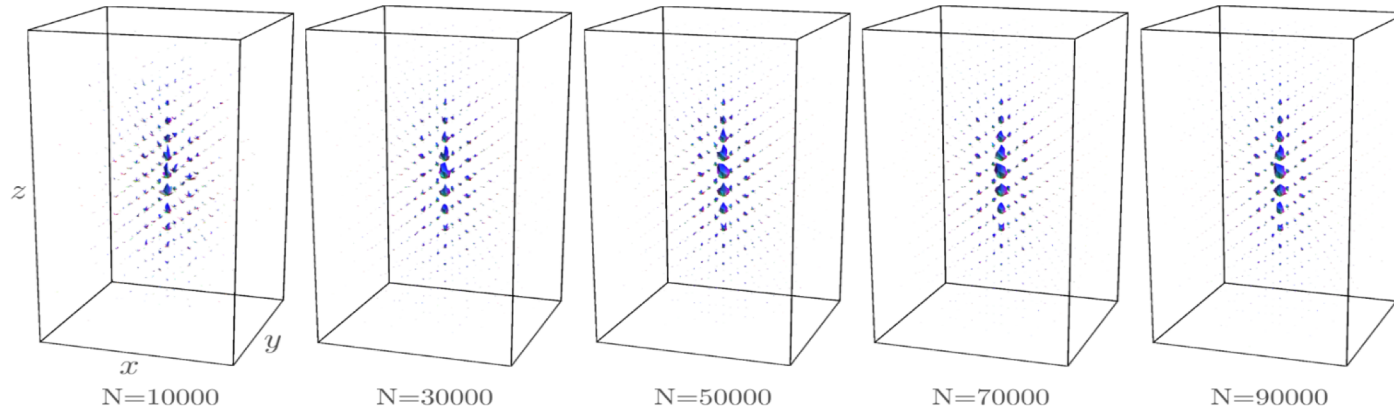
Probability kernel K_t^α for arriving at
 $(\mathbf{x}, \mathbf{n}) \in \mathbb{R}^3 \times S^2$ with traveling time t



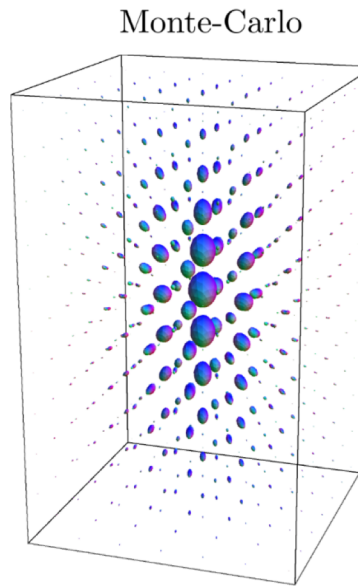
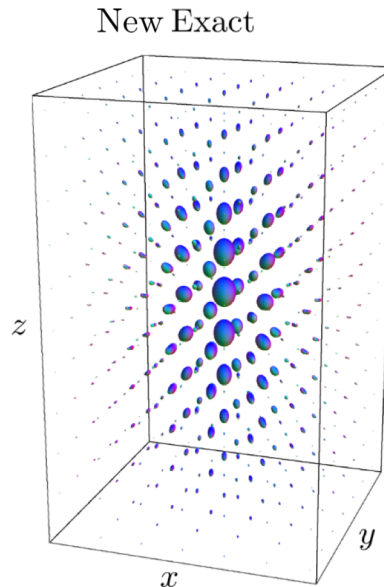
Spatial projections of random flights



Binning of end points



Entropy SI 2019



- SDEs
- Stochastic Integrals.
- Discretization.
- Binning.

$$(\mathbf{X}_M, \mathbf{N}_M) \sim \mathbf{G}_M \odot (\mathbf{0}, \mathbf{a}), \text{ with } \mathbf{G}_M = \left(\prod_{k=1}^M e^{\sum_{t=3}^5 \sqrt{\frac{t\Delta s}{M}} c_t^k A_t} \right) \mathbf{G}_0,$$

$$\lim_{N \rightarrow \infty} \lim_{\Delta s, \sigma_B \rightarrow 0} \lim_{M \rightarrow \infty} p_t^{\Delta s, \sigma_B, N, M}(\mathbf{x}, \mathbf{n}) = K_t^{x-1}(\mathbf{x}, \mathbf{n}),$$

$$\text{with } p_t^{\Delta s, \sigma_B, N, M}(\mathbf{x}, \mathbf{n}) = \sum_{l=1}^b \sum_{i,j,k \in \mathbb{Z}} 1_{c_{i,j,k}, B_l}(\mathbf{x}, \mathbf{n}) \frac{s_{ijk}^l}{M(\Delta s)^3 \sigma_B^l}.$$

Fourier Transform on \mathbb{M} (to solve linear PDEs on \mathbb{M})

Again $\tilde{U}(\mathbf{x}, \mathbf{R}) := U(\mathbf{x}, \mathbf{R}\mathbf{a})$ with $\tilde{U} \in \mathbb{L}_2(G)$ and $U \in \mathbb{L}_2(\mathbb{M})$

Let G be unimodular Lie group of type I. Then $\mathcal{F}_G(f) = ((\mathcal{F}_G f)(\sigma))_{\sigma \in \hat{G}}$ of $f \in \mathbb{L}_2(G)$ is a measurable field of bounded operators indexed by UIRs:

$$\mathcal{F}_G(f) = \int_{\hat{G}}^{\oplus} \hat{f}(\sigma) d\nu(\sigma), \text{ with}$$

$$\hat{f}(\sigma) = (\mathcal{F}_G f)(\sigma) = \int_G f(g) \sigma_{g^{-1}} dg \in B_2(\mathcal{H}_\sigma), \text{ for all } \sigma \in \hat{G},$$

$G = SE(3)$ (Mackey): $\hat{G} \leftrightarrow$ dual orbits $pS^2 \rightarrow d\nu = p^2 dp$

$$\sigma = \sigma^{p,s} : SE(3) \rightarrow B(\mathbb{L}_2(pS^2)), \quad p > 0, s \in \mathbb{Z},$$

$$\left(\sigma_{(\mathbf{x}, \mathbf{R})}^{p,s} \phi \right) (\mathbf{u}) = e^{-i \mathbf{u} \cdot \mathbf{x}} \phi(\mathbf{R}^{-1} \mathbf{u}) \Delta_s \left(\mathbf{R}_{\frac{\mathbf{u}}{p}}^{-1} \mathbf{R} \mathbf{R}_{\underline{\mathbf{R}^{-1} \mathbf{u}}} \right), \quad \mathbf{u} \in pS^2,$$

$\mathbb{M} = G/H$:

$$(\mathcal{F}_{\mathbb{M}} U)(\bar{\sigma}^{p,s}) := P_{sym} \circ \mathcal{F}_G \tilde{U}(\sigma^{p,s}) \circ P_{sym}$$

on $\mathbb{L}_2^{sym}(\mathbb{M})$:

$$\forall_{\mathbf{R} \in \text{Stab}_{SO(3)}(\mathbf{a})} : U(\mathbf{x}, \mathbf{n}) = U(\mathbf{Rx}, \mathbf{Rn})$$

The Linear PDEs of Interest: Fokker-Planck PDEs of α -Stable Lévy processes on $\mathbb{M} = G/H = \mathbb{R}^3 \rtimes S^2$

PDE on \mathbb{M} :

$$\begin{cases} \frac{\partial}{\partial t} W_\alpha(\mathbf{p}, t) = -(-Q)^\alpha W_\alpha(\mathbf{p}, t) \\ W_\alpha(\mathbf{p}, 0) = U(\mathbf{p}) \end{cases}$$

$$\begin{aligned} \alpha &\in (0, 1] \\ \mathbf{p} = (\mathbf{x}, \mathbf{n}) &\in \mathbb{M}, t \geq 0 \end{aligned}$$

$$Q = D_{11} \|\mathbf{n} \times \nabla_{\mathbb{R}^3}\|^2 + D_{33} (\mathbf{n} \cdot \nabla_{\mathbb{R}^3})^2 + D_{44} \Delta_{S^2}$$

$$D_{33}, D_{44} > 0 \text{ and } D_{11} \geq 0$$

PDE on G :

Set $\tilde{W}_\alpha(\mathbf{x}, \mathbf{R}, t) = W_\alpha(\mathbf{x}, \mathbf{R}\mathbf{a}, t)$, then

$$\begin{cases} \frac{\partial}{\partial t} \tilde{W}_\alpha(g, t) = -(-\tilde{Q})^\alpha \tilde{W}_\alpha(g, t) \\ \tilde{W}_\alpha(g, 0) = \tilde{U}(g) \end{cases}$$

$$g = (\mathbf{x}, \mathbf{R}) \in G, t \geq 0$$

$$\tilde{Q} = D_{11}(\mathcal{A}_1^2 + \mathcal{A}_2^2) + D_{33} \mathcal{A}_3^2 + D_{44}(\mathcal{A}_4^2 + \mathcal{A}_5^2)$$

Fourier Transform on \mathbb{M} for Exact Solutions to linear PDEs of Stable Levy Processes.

Duits et al. 2018 Entropy (S.I. in honor of 250th birthday of Fourier)

Theorem 1. Plancherel theorems and inversion formulas for $\mathcal{F}_{\mathbb{M}}$.

Spherodial wavefunctions: $\Phi_{\omega}^{l,m}$

Theorem 2. Spectral decompositions for PDE-evolution of α -stable Lévy-processes on \mathbb{M}

$$\mathcal{F}_{\mathbb{M}} \circ e^{-t(-Q)^{\alpha}} \circ \mathcal{F}_{\mathbb{M}}^{-1} = \int_{\mathbb{R}^+} \bigoplus_{s \in \mathbb{Z}} \sum_{l=|s|}^{\infty} e^{-(-\lambda_p^{l,s})^{\alpha} t} (\Phi_{p\mathbf{a}}^{l,s}(p^{-1}\cdot) \otimes \Phi_{p\mathbf{a}}^{l,s}(p^{-1}\cdot)) p^2 dp$$

Theorem 3. Probability kernels of α -stable Lévy processes on \mathbb{M}

- Via conjugation with $\mathcal{F}_{\mathbb{M}}$:

$$K_t^{\alpha}(\mathbf{x}, \mathbf{n}) = \frac{1}{(2\pi)^2} \int_0^{\infty} \sum_{s \in \mathbb{Z}} \sum_{l=|s|}^{\infty} e^{-(-\lambda_p^{l,s})^{\alpha} t} [\bar{\sigma}_{(\mathbf{x}, \mathbf{n})}^{p,s}]_{l,0,l,0} p^2 dp,$$

where $[\bar{\sigma}_{(\mathbf{x}, \mathbf{n})}^{p,s}]_{l,0,l,0} = \langle \sigma_{(\mathbf{x}, \mathbf{R}_n)}^{p,s} \Phi_{p\mathbf{a}}^{l,s}(p^{-1}\cdot), \Phi_{p\mathbf{a}}^{l,s}(p^{-1}\cdot) \rangle_{L_2(pS^2)}$

- Via conjugation with $\overline{\mathcal{F}}_{\mathbb{R}^3}$:

$$K_t^{\alpha}(\mathbf{x}, \mathbf{n}) = \frac{1}{(2\pi)^3} \int_{\mathbb{R}^3} \left(\sum_{l=0}^{\infty} \sum_{m=-l}^l e^{-(-\lambda_{\|\omega\|}^{l,m})^{\alpha} t} \overline{\Phi_{\omega}^{l,m}(\mathbf{a})} \Phi_{\omega}^{l,m}(\mathbf{n}) \right) e^{i\mathbf{x} \cdot \omega} d\omega.$$

TV & MC Flows on $\mathbb{M} = SE(d)/H$

$$\begin{aligned}
 \frac{\partial W^\varepsilon}{\partial t}(\mathbf{p}, t) &= \left(\|\nabla W^\varepsilon(\mathbf{p}, t)\|^2 + \varepsilon^2 \right)^{\frac{a}{2}} \left(\operatorname{div} \circ \frac{\nabla W^\varepsilon(\cdot, t)}{(\|\nabla W^\varepsilon(\cdot, t)\|^2 + \varepsilon^2)^{\frac{b}{2}}} \right)(\mathbf{p}) \\
 0 &= \mathbf{N}(\mathbf{x}) \cdot \nabla_{\mathbb{R}^d} W^\varepsilon(\mathbf{x}, \mathbf{n}, 0) \quad \mathbf{p} = (\mathbf{x}, \mathbf{n}) \in \partial\Omega \\
 W^\varepsilon(\mathbf{p}, 0) &= U(\mathbf{p}) \quad \mathbf{p} = (\mathbf{x}, \mathbf{n}) \in \Omega \subset \mathbb{M}
 \end{aligned}$$

$(a, b) = (0, 0)$: diffusion

$\varepsilon \geq 0$ $(a, b) = (0, 1)$: TV — Chambolle et al. 2018.
 $(a, b) = (1, 1)$: MCF — Citti et al. 2016.

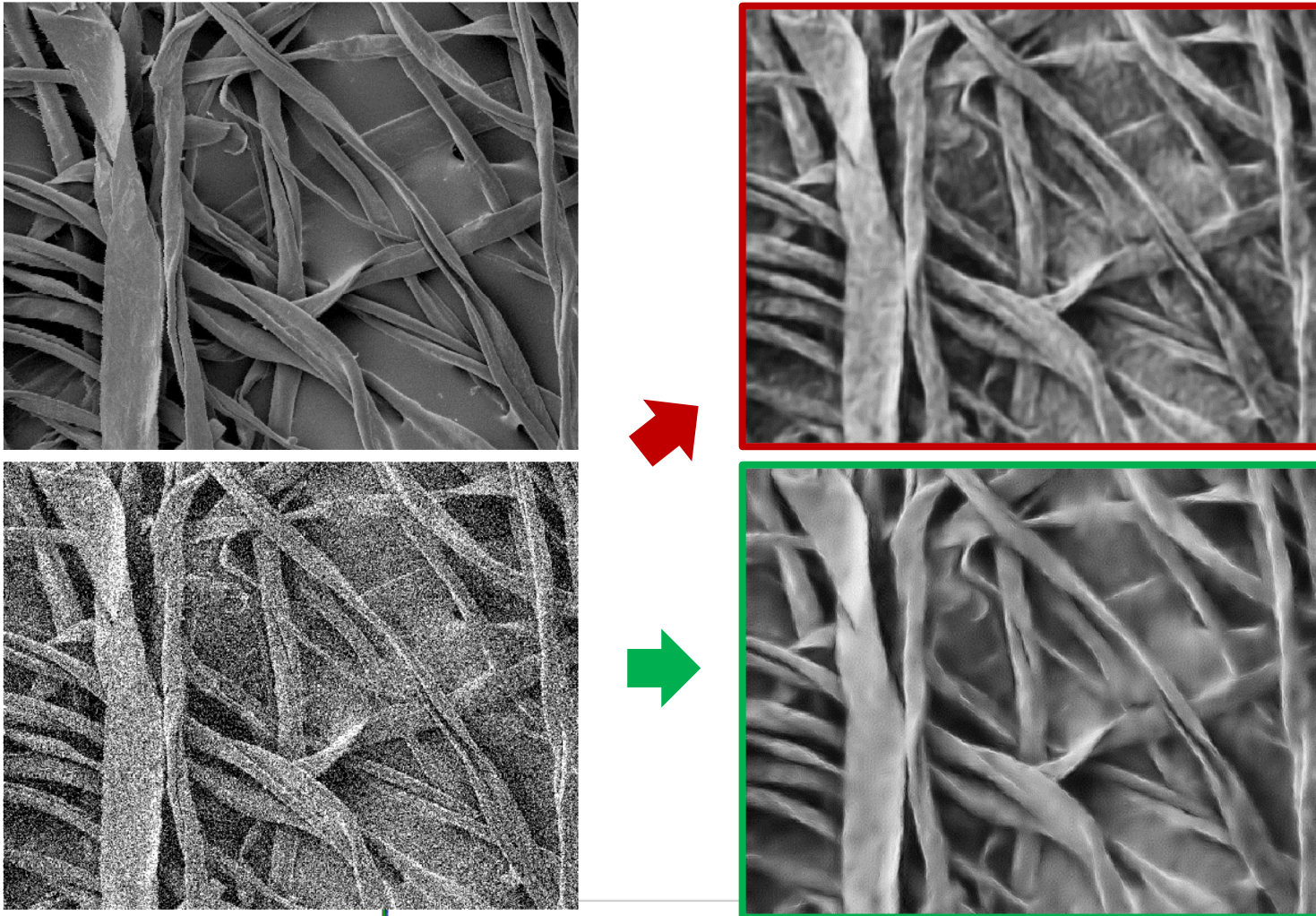
$$\text{For } U \in BV(\Omega) \quad : \quad TV_\varepsilon(U) := \sup_{\substack{\psi \in C_c^\infty(\Omega) \\ \mathbf{v} \in \chi_0(\Omega) \\ \|\mathbf{v}(\mathbf{p})\|^2 + |\psi(\mathbf{p})|^2 \leq 1}} \int_{\Omega} \binom{\varepsilon}{U(\mathbf{p})} \cdot \binom{\psi(\mathbf{p})}{\operatorname{div} \mathbf{v}(\mathbf{p})} d\mu(\mathbf{p})$$

$\partial TV_\varepsilon(U)$ is closed, convex. $\rightarrow \operatorname{grad} TV_\varepsilon(U)$

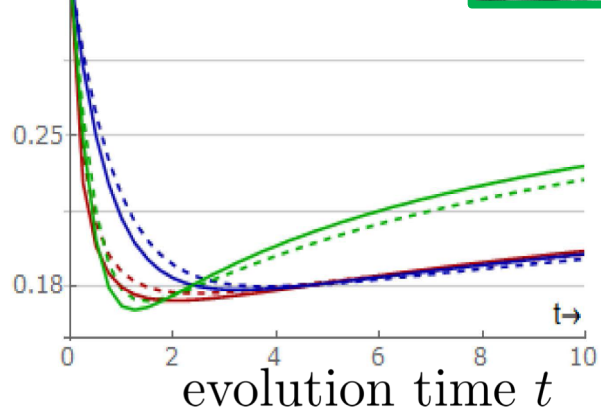
Gradient flow: $\exists!$ W^ε abs. cont. : $\frac{\partial W^\varepsilon}{\partial t} = -\operatorname{grad} W^\varepsilon$ & $\lim_{t \downarrow 0} W^\varepsilon(\cdot, t) = U$.

Theorem (convergence)

$$\|W^\varepsilon(\cdot, t) - W^0(\cdot, t)\|_{\mathbb{L}_2(\Omega)} \leq 8 \left(\|U\|_{L^2(\Omega)} (TV_0(U) + \delta) \delta t^2 \right)^{1/5} \text{ with } \delta = \varepsilon |\Omega|$$



\mathbb{L}_1 -error



- Left Invariant CED-OS
- - - Left Invariant TVF-OS
- · - Left Invariant MCF-OS
- Gauge Frame CED-OS
- Gauge Frame TVF-OS
- Gauge Frame MCF-OS

Real Data

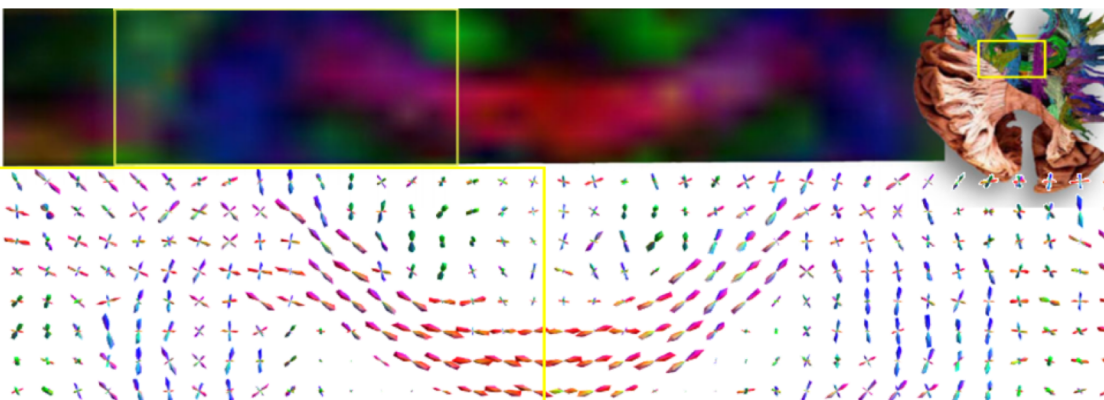
Scanner settings:

$$b = 1000 \text{ s/mm}^2$$

$$N_o = 54$$



FODF:
CSD
(inverse problem)



on \mathbb{M}

Diffusion

Linear

CED

PM

$$K=0.2$$

TVF

$$\epsilon=0.02$$

MCF

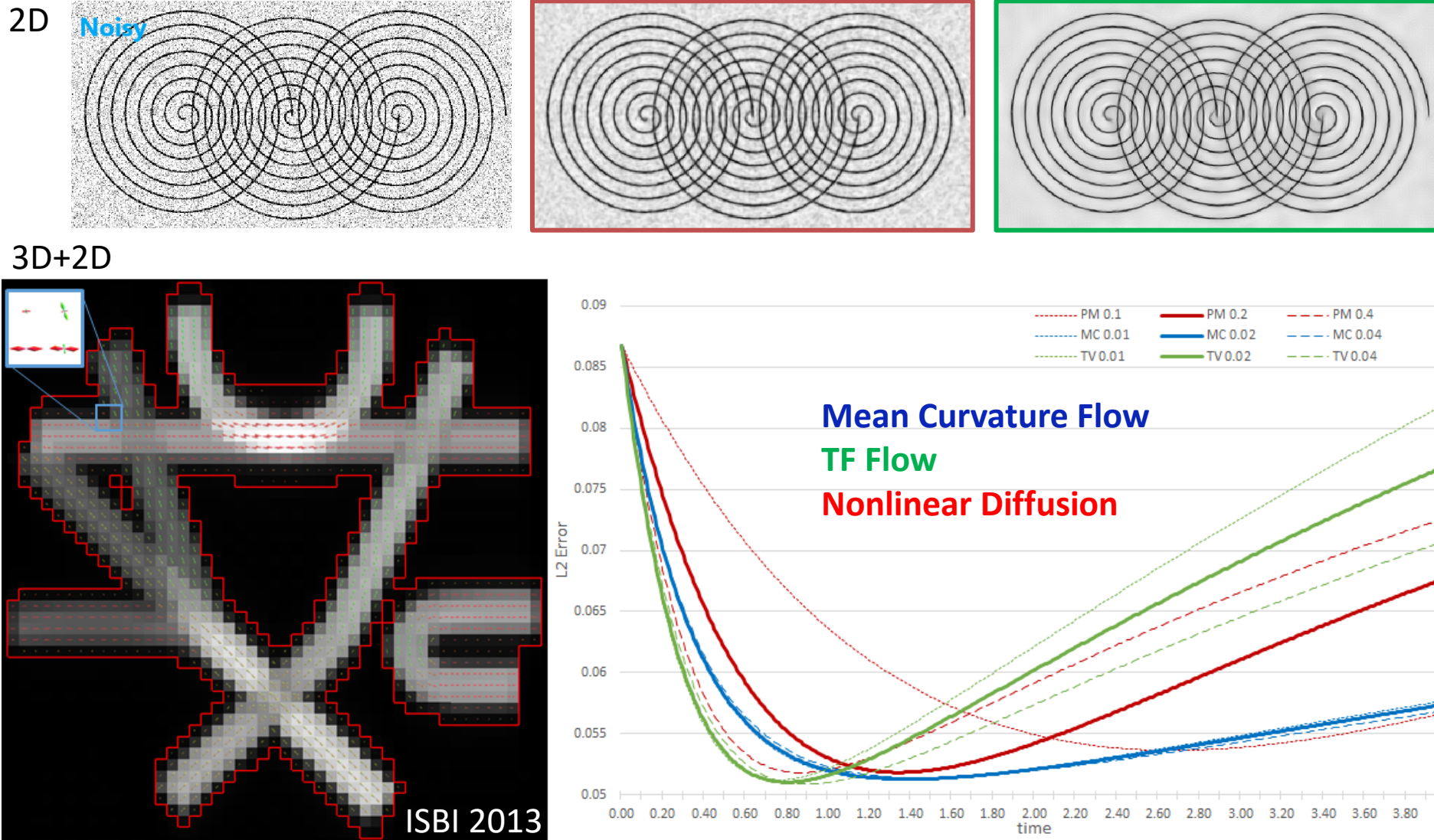
$$\epsilon=0.02$$

Nonlinear

Total Variation

Mean Curvature Flow

Evaluation Denoising on Phantoms



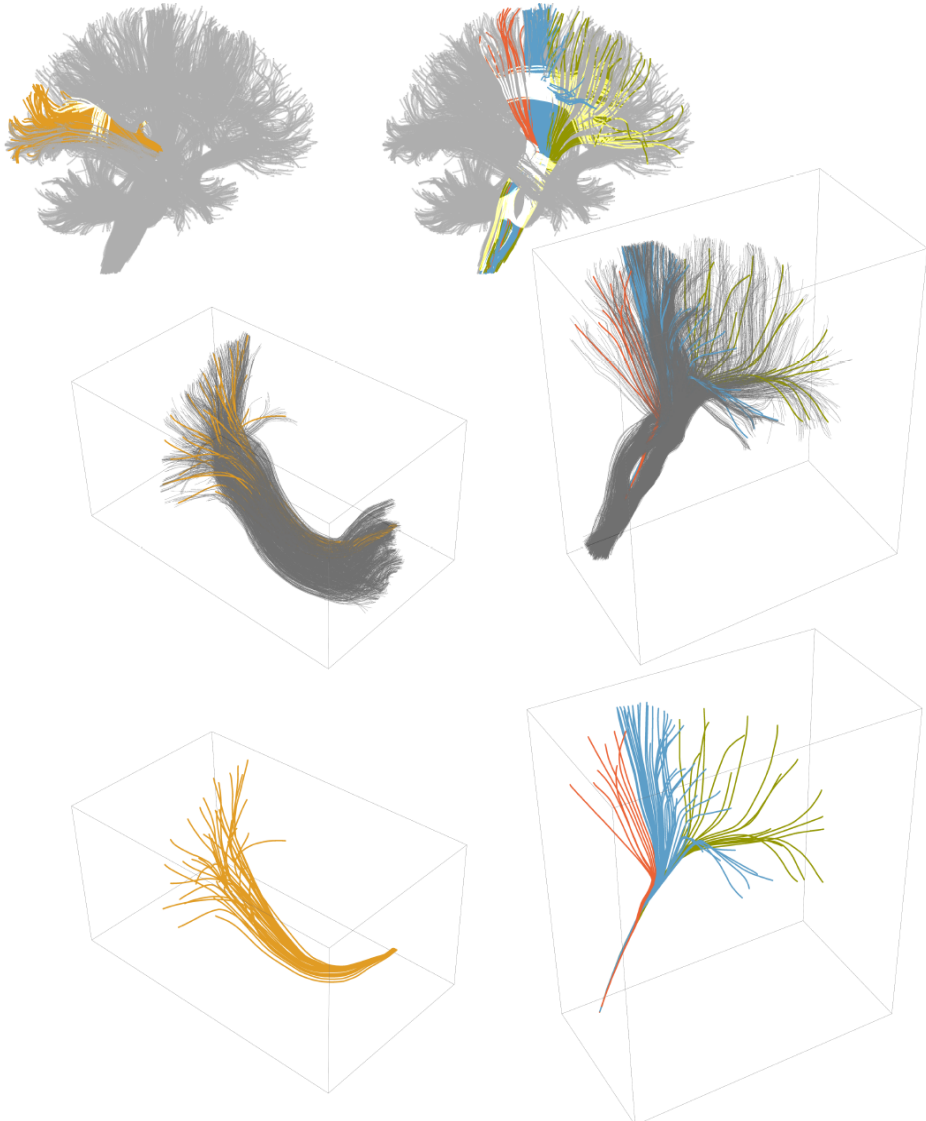
TF Flow: preserves boundaries and plateaus and minimal results for t^* but stability issues.

Nonlinear Diffusion: OK but relatively unstable w.r.t. pars and t .

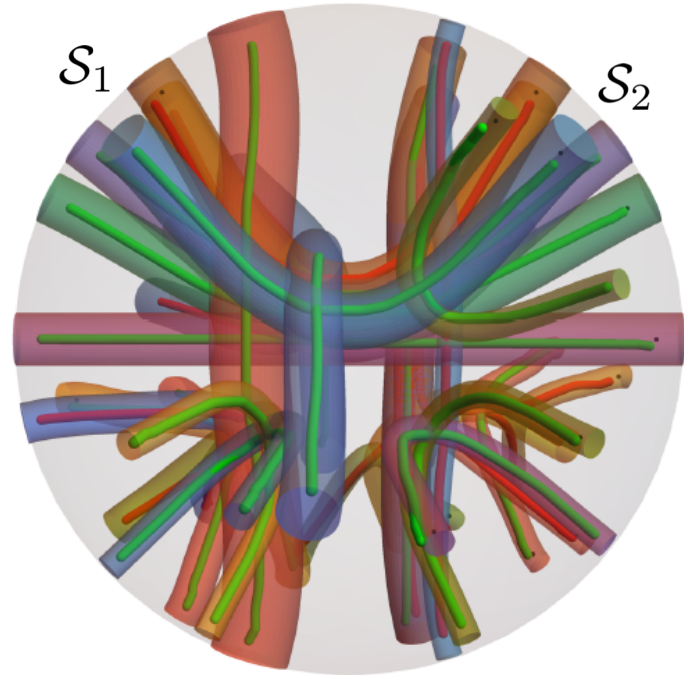
Mean Curvature Flow: low errors for all t , best preservation of crossings, and most stable.

Geodesic Tracking and Geodesic Connectivity in DW-MRI

Deterministic tracking (ISMRM 2017)
that deals with crossings and parallel fibers



Connectivity measures (ISBI 2013)
without tracking



$$\begin{aligned} c(\mathcal{S}_1, \mathcal{S}_2) &= \max\{ \bar{c}(\mathcal{S}_1, \mathcal{S}_2), \bar{c}(\mathcal{S}_2, \mathcal{S}_1) \}, \\ \bar{c}(\mathcal{S}_1, \mathcal{S}_2) &= \frac{1}{|\mathcal{S}_2|} \int_{\mathcal{S}_2} w(\mathbf{q}) \max_{\mathbf{p} \in \mathcal{S}_1} \left\{ \frac{\mathcal{E}(\mathbf{p}, \mathbf{q})}{d_{\mathcal{F}}(\mathbf{p}, \mathbf{q})} \right\} d\mathbf{q} \\ \mathcal{E}(\mathbf{p}, \mathbf{q}) &= \int_0^1 \sqrt{\xi^2 |\mathbf{x}'(t) \cdot \mathbf{n}(t)|^2 + \|\mathbf{n}'(t)\|^2} dt \end{aligned}$$

(MICCAI-DCMRI 2019)

Conclusion

- Current vessel tracking and enhancement in CAD-tools fail at complex structures, and this can be tackled via orientation scores of images.
- We solved many PDEs on $\mathbb{M} = \mathbb{R}^d \times S^{d-1} := SE(d)/H$:
 - new exact solutions to:
 - all linear convection-diffusions (DGA 2017)
 - Fokker-Planck PDEs of Lévy Processes (Entropy 2019 SI to honor Fourier)
 - Sub-Riemannian geodesics for d=3 (JDGS 2016)
 - new numerical solutions (with analysis + convergence thms) to:
 - nonlinear diffusion (IJCV 2009, QAM 2010, JMIV 2018)
 - TV & MC flows (SSVM 2019)
 - Eikonal PDEs for sub-Riemannian front propagation (SIAM 2016, JMIV 2018)
prior to: optimal (cusp-free) paths in orientation scores
- We tackled many medical imaging applications: fiber/vessel enhancement, tracking & connectivity, in 2D-3D Data and in 5D DW-MRI.